AN ALTERNATE APPROACH TO QUANTUM CHAOS THROUGH BOHMIAN MECHANICS

SEAN NIEUWENHUIS
Bachelor of Science, University of Lethbridge, 2022

A thesis submitted
in partial fulfilment of the requirements for the degree of

MASTER OF SCIENCE

in

PHYSICS

Department of Physics and Astronomy
University of Lethbridge
LETHBRIDGE, ALBERTA, CANADA

AN ALTERNATE APPROACH TO QUANTUM CHAOS THROUGH BOHMIAN MECHANICS

SEAN NIEUWENHUIS

Date of Defence: April 3, 2024

Dr. Saurya Das Thesis Supervisor	Professor	Ph.D.
Dr. Mark Walton Thesis Examination Committee Member	Professor	Ph.D.
Dr. Ken J.E. Vos Thesis Examination Committee Member	Associate Professor	Ph.D.
Dr. Slaven Peles External Thesis Committee Member Oak Ridge National Laboratory	Senior Computational Scientist	Ph.D.
Dr. Chad Povey Chair, Thesis Examination Committee	Instructor III	Ph.D.

Dedication

I dedicate this work to my parents, Dave and Sharon Nieuwenhuis.

Abstract

The development of quantum mechanics has proven to be one of the most revolutionary and important descriptions of the universe at its most fundamental scale, but there remains much work to be done for a complete description of all physical phenomena. One notable area of research focuses in the realm of quantum chaos and the lack of a clear correspondence between a classical and quantum description of chaos.

Taking a step back from the usual interpretation of quantum mechanics in terms of a wavefunction and its collapse, we study an alternate but correct description of quantum mechanics via the so-called Bohmian picture, with implications for quantum chaos. The resultant description is in terms of 'Bohmian trajectories', which are nothing but quantum counterparts of classical trajectories. We will demonstrate that this alternate interpretation can provide a new description of quantum chaos, with a much clearer correspondence to its classical counterpart.

Acknowledgments

First, I would like to thank my supervisor Dr. Saurya Das for his assistance and encouragement throughout the entirety of my M.Sc. program. He was a true pleasure to work with, and this work could not have been completed without his tremendous support.

I would like to thank my parents Dave and Sharon, my brother Joshua, and my sister Sara for their continuous encouragement throughout my program, as well as providing relief during the more stressful moments. I would not have been able to focus on this research if they were not supporting me every step along the way.

Finally, I would like to thank the other graduate students at the time of my M.Sc. program, specifically Dr. Mitja Fridman[1], Mustafa Amin, Narasimha Gosala, and Juan Lopez. Whether we were discussing our work and challenging each other, or simply taking a break over lunch, they have always provided encouragement and useful suggestions as well as pleasant breaks when they were needed most.

[1] Completed his Ph.D during the time of my program

Table of Contents

List of Figures

Chapter 1
Introduction

Throughout the pursuit of human knowledge and understanding, a common goal has often been to develop concise and predictable descriptions of observable phenomena. One of the most famous and successful works was completed by Isaac Newton in 1687 where the concepts of mechanics were fully developed [4], now referred to as 'classical mechanics'. This has since been improved upon with the introduction of quantum theory, in which classical mechanics is no longer sufficient to describe the behaviour of the system and leading to the development of quantum mechanics [5]. These systems often emerge as length scales begin to transition from macroscopic (classical mechanics) to microscopic (quantum mechanics).

As there exists an apparently continuous spectrum of possible length scales within the physical world, one would expect that a complete description of a system should include both classical and quantum descriptions, where either theory will become more dominant in specific regions. In this sense, all systems could expectantly become quantum at their fundamental length scales, with this quantum description often becoming negligible as they approach the classical region. While this is not an exact rule for all cases as certain macroscopic systems are described in terms of quantum mechanics, such as magnets, it remains a useful generalization to describe a majority of systems. It is this idea that formed the basis of Bohr's correspondence principle, stating that the classical picture will emerge in the limit commonly discussed as $\hbar \to 0$ [6–10]. In terms of probability as is often discussed in quantum mechanics, the Heisenberg uncertainty relation $\Delta X \Delta P_x \geq \hbar/2$ [11] would reduce to the momentum and position distributions decreasing to an infinitely narrow width [12]. The

uncertainty then reduces and becomes negligible as is the case for classical measurements.

But what happens at the intermediate length scales, where the classical and quantum regimes meet? It is not entirely clear as to which theory best describes the occurring phenomena. Additionally, there is often no clear length scale at which the system transitions from classical to quantum. This problem arises in the description of chaos theory. As explained in more detail in the following chapters, the usual descriptions and measurements differ in such a way that a classical limit does not appear to rise from the quantum mechanical description, as one would expect from Bohr's correspondence principle. In fact, the common understanding and descriptions of quantum chaos have even led for some to question this correspondence principle, with some attempts for reinterpretation of this correspondence [13]. Consider however, that this disagreement may not necessarily result from the physical phenomena present in quantum mechanics, but may instead be specific to its interpretation. In this case, an alternate interpretation of quantum mechanics may resolve this issue and potentially provide additional insight into the classical limit of quantum mechanics.

While the Copenhagen interpretation is the most popular, and arguably more useful, interpretation of quantum mechanics, others exist that can provide complementary pictures with the same predictions for measurable quantities. They take in the same ingredients and provide the same predictions, but with differences in the intermediate quantum behaviour of the system. This can then provide a considerable amount of freedom in choosing an interpretation to work with, so long as the predictions are not invalidated by any measurable phenomena. To investigate how this may affect the understanding of chaos theory, suppose that there exists an alternate interpretation of quantum mechanics in which classical mechanics appears more clearly as a limit of quantum mechanics. One would then be wholly justified in choosing such an interpretation to describe chaos in quantum mechanics to determine if

such a classical limit would also apply in chaos theory. In order to test this, consider two classical potentials which have previously been studied and shown to demonstrate chaos as discussed in Chapter 2. Then considering quantum chaos in the standard interpretation of quantum mechanics as discussed in Chapter 3, identify how quantum chaos is analyzed and quantified. These descriptions rely on the Heisenberg picture of quantum mechanics to explain operator growth as a function of time, which is not clearly analogous to the classical descriptions of chaos in terms of trajectories. With these two distinct descriptions, one can consider an alternate, but completely correct, interpretation of quantum mechanics that describes quantum effects resulting from a quantum potential, as discussed in Chapter 4. This interpretation, namely the Bohmian interpretation, then describes quantum behaviour in terms of Bohmian trajectories that result from this quantum potential.

Using the Bohmian interpretation of quantum mechanics, specific quantum potentials are then chosen to (identically) mimic the previously mentioned classical potentials. As these quantum potentials directly result from the wavefunction amplitude, these amplitudes can be solved (as in Chapter 5) in order to determine if they are physically valid solutions that could ideally be reproduced in a suitable laboratory. By choosing a 'free' particle so that it is only under the influence of this quantum potential, its Bohmian trajectories should behave chaotically analogous to the corresponding classical trajectories. Since these are all purely quantum effects, such behaviour, if it were to exist, could be understood as a form of quantum chaos. It is this description of quantum chaos that will be developed and discussed as the objective of this work.

Chapter 2
Classical Chaos

2.1 Standard Quantities and Representations

When describing the mechanics of the macroscopic world, one of the most fundamental and useful descriptions arises in terms of trajectories, where the evolution of the system can be described for any position and time [14, 15]. With this, a system can be described using a well-defined 'path' between its initial and final positions containing a complete description of observable parameters at any position and time along this path. This description is often of the form of Newton's second law of motion, which relates the system's velocity to potential as

$$m\frac{d\vec{v}}{dt} = -\vec{\nabla}V \tag{2.1}$$

which can then provide the expression for the position at any time. Clearly from this description in terms of a differential equation, the evolution of a system is dependent on its previous state, with this dependence remaining for every successive state.

With this dependence of trajectories on previous states, a new description of natural phenomena arises as certain systems may become heavily dependent on these states, recurring back to the initial conditions of the systems. By altering the initial conditions of the system *very slightly*, the final state can become *extremely* different than it would have been with the original set of initial conditions as discussed in Chapter 11 of [15] and Chapter 4 of [14]. Behaviour of this form results from the dynamics of nonlinear systems [14, 15] and have since been classified as chaotic systems, referring to their *apparent* unpredictability of the resultant trajectories. One notes that while in some instances, an analytical solution of

the equation can be found, in the vast majority of cases one has to resort to numerical methods. This class of systems are specifically referred to as 'deterministic chaos' to distinguish it from 'randomness', however this will be referred to as simply 'chaos' for the following discussions. In addition to this sensitivity to initial conditions, these systems display notable behaviour within its own state space. By selecting some finite region of initial states, the time-evolution of this region can cause it to pass over every available state within the space, generally referred to as global mixing [16]. These conditions of sensitivity to initial conditions and global mixing are strong indicators of chaotic behaviour individually, but both are necessary for a system to be classified with certainty. In fact, these systems arise often in natural processes, with examples in weather patterns and planetary motion [14]. With such a natural occurrence of chaotic systems, the need then arises for some measure of this sensitivity to initial conditions, to understand and describe how chaotic these systems are.

As chaotic trajectories are described in terms of the difference of final states depending on changes of initial states, one may choose to describe how chaotic a system is by quantifying this difference in states. This would then depend on the difference between the states after some time $\delta x(t)$ and the difference between the initial states $\delta x(0)$. The mean growth rate of the distance between trajectories can then be represented as $|\delta x(t)|/|\delta x(0)|$ as in Chapter 6 of [16], with the distance between trajectories as [15]

$$s(t) \sim s_0 e^{\lambda t} \ , \tag{2.2}$$

where s_0 is the initial separation of the trajectories and λ is referred to as the Lyapunov exponent, calculated as [16]

$$\lambda \approx \frac{1}{t} \ln \frac{|\delta x(t)|}{|\delta x(0)|} \ . \tag{2.3}$$

From its definition in terms of the natural logarithm, the descriptive power of the Lyapunov

exponent arises through its sign. If the trajectories are diverging, that is $|\delta x(t)| > |\delta x(0)|$, then the system will be considered as chaotic and the Lyapunov exponent $\lambda > 0$ (as discussed in Chapter 3 of [17] and Chapter 4 of [14]). Alternatively, the trajectories can either converge or remain equally separated, that is $|\delta x(t)| \leq |\delta x(0)|$, resulting in a stable system with the Lyapunov exponent $\lambda \leq 0$.

As systems become more complex however, often due to an increasing number of degrees of freedom, trajectories can become much more complicated resulting in great difficulty when studying Lyapunov exponents. Instead, consider the motion of the system in phase space, where the observer records the contact of the motion with some phase space cross-section [15, 17, 18]. The resulting maps of intersection points are referred to as Poincaré sections where the complexity of the curve represents any chaotic or non-chaotic behaviour. A chaotic system will display as an irregular and random distribution of intersection points with the phase space cross section. The opposite remains true as well, where a simple and closed curve represents a system within a region of stability. It is also important to note that for a system that creates periodic curves in phase space, the Poincaré section can also appear as a collection of points rather than a closed curve [18]. By observing the periodicity of the cross-section intersection, or the lack thereof, insight can be gained into the behaviour of these trajectories through visual representation, but a trade-off is now introduced as this does not provide a clear quantitative measurement of the chaotic behaviour. It remains open to the observer to distinguish where chaotic regions may occur rather than providing a single measurement that leaves little room for dispute.

This phase space representation of chaotic behaviour also introduces the concept of attractors. After some evolution in time, a fixed point or stable orbit in phase space to which a stable system approaches is referred to as an attractor [14, 15]. A simple example of this is a damped pendulum about a fixed point. As the pendulum evolves over some period in

time, the magnitude of the oscillation will decrease until it eventually rests at its lowest point. Observing this trajectory in phase space would show a continuing attraction towards this rest position, making this point an attractor. In a chaotic system however, these attractors may not be local within a given region of phase space. These attractors, referred to as strange attractors, can be dispersed throughout phase space [14, 15] and therefore result in the irregular behaviour of chaotic trajectories in phase space [18]. An example of this can be seen in the later discussion of the Hénon-Helies Hamiltonian in Section 2.3.

With this understanding of how chaos is represented in classical mechanics, as well as two of the more common methods of measuring chaos within a system, consider next two systems that have been well-studied and understood to display classically chaotic tendencies. By studying these systems in classical mechanics, focusing on the potential of the systems and the parameters that induce chaotic behaviour in the classical trajectories, the behaviour can then be understood with the intention of further consideration in later chapters.

2.2 The Parametric Oscillator

Consider first a simple example of chaos in classical mechanics, namely the parametric oscillator in one dimension as represented in Chapter 11 of [15]. This system occurs when a simple harmonic oscillator is subject to a periodic oscillation of its equilibrium point so that the frequency of oscillation is now a time-dependent parameter. A simple example of this model could be a pendulum with the length of the pendulum arm oscillating in addition to the swinging of the pendulum itself. The equation of motion would then be quite similar to that for the simple harmonic oscillator, but the natural frequency will be replaced with a time-dependent frequency, resulting in [19–22]

$$\frac{d^2}{dt^2}x + \omega^2(t)x = 0\ . \tag{2.4}$$

In the case where this time-dependent frequency differs very slightly from the natural frequency and takes the form of a periodic function, it can be expressed as

$$\omega^2(t) = \omega_0^2[1 + h\cos(\gamma t)] \tag{2.5}$$

following Chapter 5 of [23].The strength of this time-dependence is clearly dependent on the parameter[2] h , where $h \ll 1$ can be chosen as a perturbation coefficient. One writes $\gamma = 2\omega_0 + \varepsilon$ since the parametric resonance has the greatest effect when the frequency of this oscillation is close to $2\omega_0$, with the additional condition $\varepsilon \ll \omega_0$ to introduce a slight difference in frequency between the oscillations [23]. This additional perturbation term acts multiplicative to the variable x creating a nonlinear system, increasing the dependence on initial conditions and resulting in a chaotic system [21]. Using Newton's law of motion, the potential for Eq. (2.4) can be read-off as

$$V = \frac{1}{2}k[1 + h\cos(\gamma t)]x^2 \tag{2.6}$$

where $k = m\omega_0^2$. This result clearly returns the form of a simple harmonic oscillator with an additional perturbation term dependent on the magnitude of the parameter h. Interestingly, the Lagrangian takes a similar form, but with an additional nonlinear term as

$$\mathcal{L} = \frac{1}{2}m\dot{x}^2 - \frac{1}{2}kx^2 - \frac{1}{2}kh\cos(\gamma t)x^2 \tag{2.7}$$

where h clearly introduces or removes the additional modulation away from the simple harmonic oscillator. While this Lagrangian form is not specifically used in following consideration, it is worth identifying its key features. Depending on the magnitude of this parameter h, the system can approach the simple harmonic oscillator and behave in a stable manner, or it will exhibit chaos [20, 21] as this modified oscillation introduces a nonlinear term that

[2]Note that this is not the same as Planck's constant h

will increase the dependence on the initial state [14]. Following the methodology of [24], the Lyapunov exponents can be computed and plotted for various cases of the parametric oscillator system. For a stable system, for example $k = 1$ and $h = 0$, such that the system is a simple harmonic oscillator, the Lyapunov exponents can be seen in Fig. (2.1) to be less than zero. Considering next the system with $k = 1$ and $h = 1$, the Lyapunov exponents can be seen in Fig. (2.2) to be greater than zero, and the system will be chaotic.

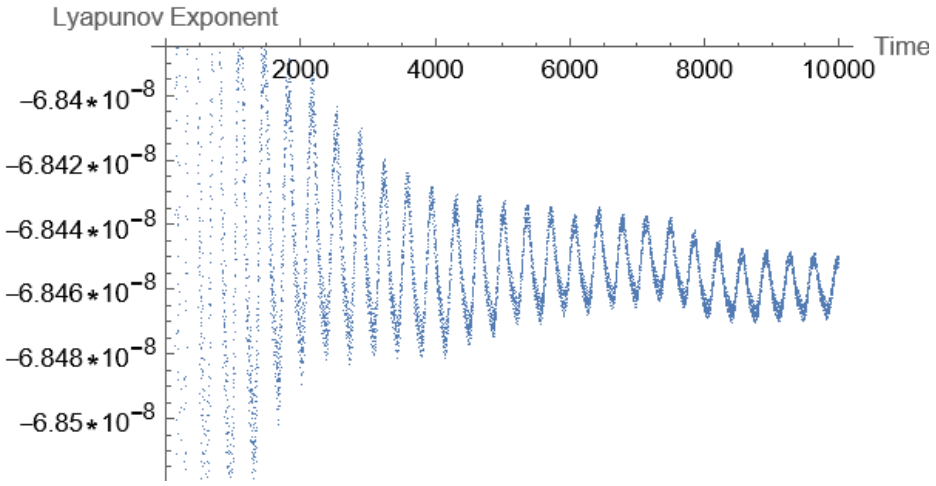

Figure 2.1: The Lyapunov exponents for the parametric oscillator system, with $k = 1$ and $h = 0$.

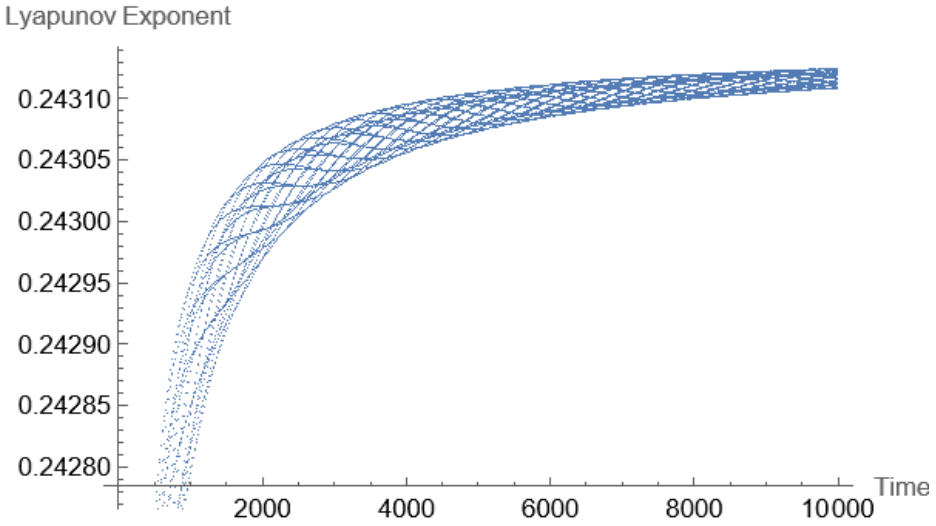

Figure 2.2: The Lyapunov exponents for the parametric oscillator system, with $k = 1$ and $h = 1$.

2.3 The Hénon-Heiles Hamiltonian

While simple cases working in one dimension are ideal systems for analysis, the vast majority of systems in nature work in either two or three dimensions. Take for example the orbit of Earth around the Sun. The orbit is often explained and analyzed in two dimensions, that is an orbit in some plane of space, but in reality the entire system is also moving through a third dimension in space. Even though all three dimensions are required for a complete description, the actual orbit can be sufficiently described using just two. Indeed, two-dimensional systems have been shown to work very well in many situations to describe the natural world, so it is justified to take the previously mentioned description of chaos to a second dimension.

As for the one-dimensional case, consider a two-dimensional system that takes the form of a simple harmonic oscillator with an additional higher order perturbation term. One of the simplest systems of this type is the Hénon-Heiles Hamiltonian [2] with the potential expressed as [15, 25]

$$V = \frac{1}{2}k(x^2+y^2) + h\left(x^2 y - \frac{1}{3}y^3\right) , \tag{2.8}$$

where $k = m\omega_0^2$ and h determines the strength of perturbation as was the case for the parametric oscillator potential in Eq. (2.6). The analysis for this system is often considered in terms of the dimensionless energy where $k, h = 1$ to understand how increasing the energy of the system will affect its behaviour. As represented in Fig. (2.3), the motion is bounded for the dimensionless potential $V \leq 1/6$ where the trajectories will become less stable as the energy increases up to this critical value $V = 1/6$ [26]. Beyond this potential, the motion will be unbounded and the (perturbed) oscillatory motion will no longer occur [15, 26]. The intersection points of the triangle for $V = 1/6$ in Fig. (2.3) then represent saddle points in the contour causing unstable equilibrium, with a single point of stable equilibrium at the origin $(x, y) = (0, 0)$ [1, 26, 27].

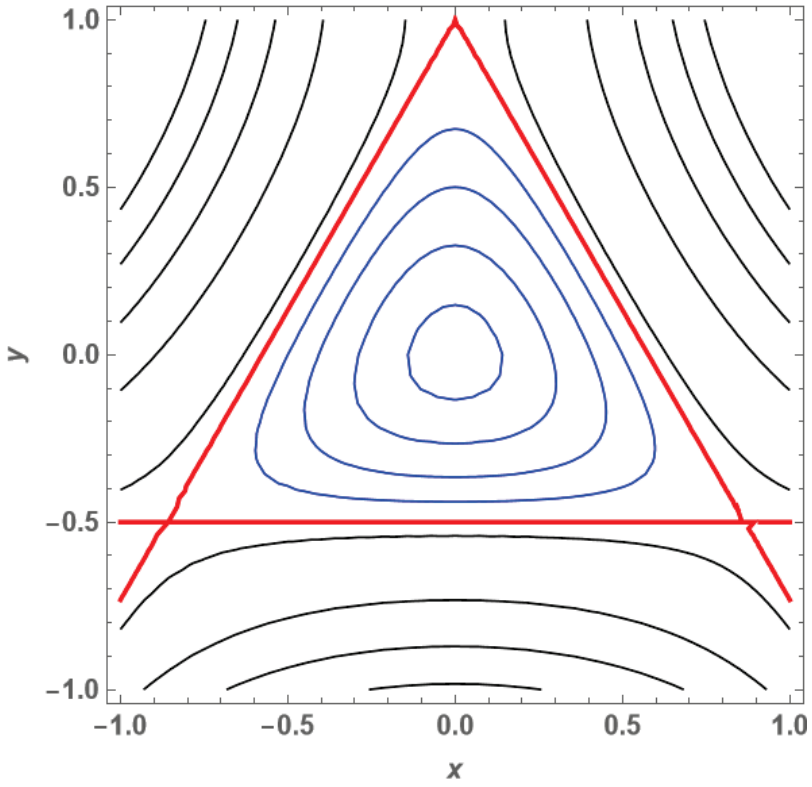

Figure 2.3: The equipotential lines of the Hénon-Heiles Hamiltonian, with $h,k = 1$. The blue contour lines represent bounded motion for $V < 1/6$, the red contour line represents the maximum potential $V = 1/6$ for bounded motion, and the black contour lines represent unbounded motion for $V > 1/6$. Adapted from [1].

Note that the chaotic behaviour of the system relies on the magnitude of the potential, which depends on the parameters k and h. The chaotic behaviour must then depend on the magnitude of h in comparison to k. In the case that $h \ll k$, the simple harmonic behaviour would dominate and the system would be stable. It is only when h increases to the point that the perturbation is no longer negligible that the system transitions away from the harmonic oscillator and its behaviour turns chaotic. Recall that h was also the parameter which determined whether the parametric oscillator was chaotic or not, in the previous example. To understand the behaviour of the system as h becomes dominant, consider multiple cases of increasing h to observe the Poincaré plots. These can be created by following the procedure and initial conditions provided by [28], with a modification so that the variable h can be altered to observe its effects. In the case where both $k,h = 1$, the system can be observed

to exhibit stable behaviour as created and represented in Fig. (2.4). The trajectory will pass through the phase space cross-section in a repetitive nature to create closed orbits, with each orbit resulting from a different set of initial conditions. Alternatively the case where $k = 1$ and $h = 1.4128$ can cause the system to behave chaotically as created and represented in Fig. (2.5). For a variety of initial conditions, there appear to be very few closed orbits caused by the trajectories passing through the phase space cross-section with the majority passing through at what appear to be random points, restricting the predictive capacity of these trajectories.

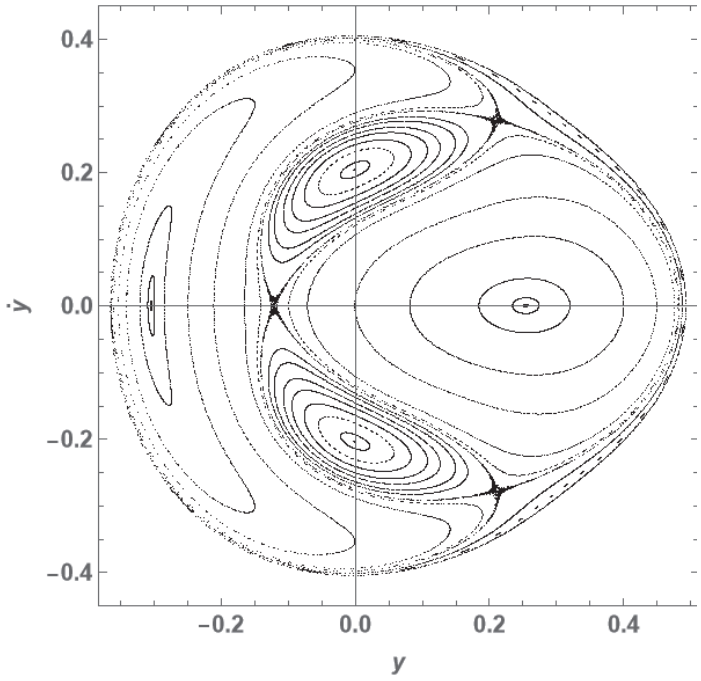

Figure 2.4: Poincare section of the Hénon-Heiles system for a variety of trajectories with different initial conditions, with $k, h = 1$. Adapted from [2].

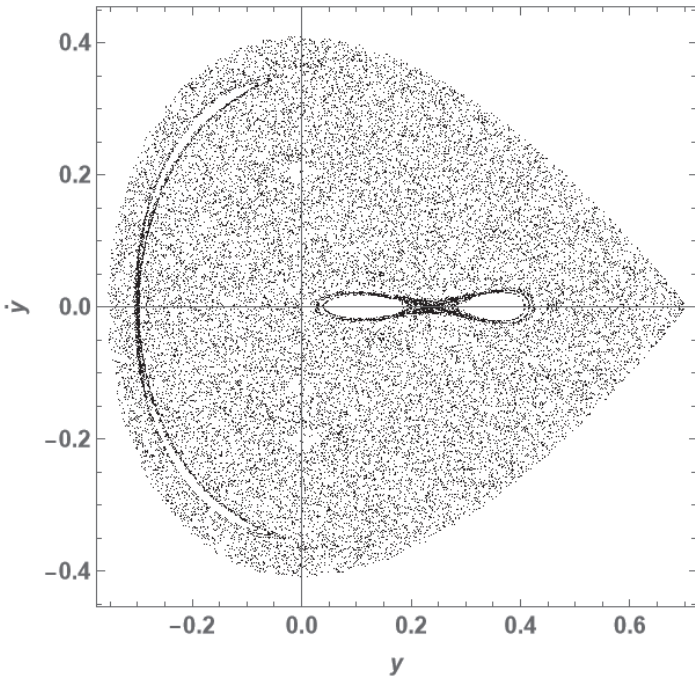

Figure 2.5: Poincare section of the Hénon-Heiles system for a variety of trajectories with different initial conditions, with $k = 1$ and $h = 1.4128$. Adapted from [2].

Chapter 3

Common Descriptions of Quantum Chaos

With these well-understood methods for describing chaos in classical dynamics, one would naturally think as to how this may translate into quantum mechanics, given that our world is fundamentally quantum and its classical description, when applicable, arises as an approximation. This motivates one to anticipate that there must be a description of chaos in terms of quantum mechanics in order to provide a fundamental basis for the classical behaviour, consistent with Bohr's correspondence principle [29]. This has led to several attempts to formulate such a description, explained more specifically in the following sections.

3.1 Quantization and Semiquantum Chaos

One potential way to formulate a description of quantum chaos is via the quantization of a classical system that demonstrates chaos [29]. This process often begins with the standard rule for quantization where momentum is expressed as an operator in position space [6, 9, 12, 30] with

$$P_x = -i\hbar\frac{\partial}{\partial x}\,, \tag{3.1}$$

considering one dimension in space (x) for simplicity. Additionally, for a quantum system now described in terms of a wavefunction $\psi(x,t)$, the time-evolution is expressed by the Schrödinger equation

$$H\psi(x,t) = i\hbar\frac{\partial}{\partial t}\psi(x,t) \tag{3.2}$$

where the Hamiltonian H, if non-relativistic, takes the form

$$H = \frac{P_x^2}{2m} + V(x) = -\frac{\hbar^2}{2m}\frac{\partial^2}{\partial x^2} + V(x) \tag{3.3}$$

for an arbitrary potential $V(x)$. In order for the wavefunction to be a physically valid solution of the Schrödinger equation, it is generally required to be bounded within the available region of x. If not, it could increase in magnitude indefinitely and the probability density $|\psi|^2$ would have no meaning. While there are systems in which the wavefunction can be infinite while still resulting in a total probability of unity, these are rare and special cases. With this, the following discussion will focus on the previously stated generalization. Additionally, this gives rise to a restriction on the allowed energy states within the bounded system, in that there are often discrete energy values that will satisfy the equation given its initial conditions. When the discrete energy levels result from a bounded system, the wavefunction demonstrates quasiperiodic dynamics [31], which makes exponential divergence of trajectories highly improbable. This therefore removes the possibility for chaos in the wavefunctions within the quantum mechanical system. The behaviour holds for all bounded quantized systems, regardless of the stable or chaotic dynamics of the corresponding classical system [29]. Additionally, the alternate study of the semiclasssical limit of quantum systems, specifically as $\hbar$ and quantum effects are small but cannot be ignored, and where the classical counterpart exhibits chaotic behaviour is referred to 'quantum chaology' [32], in order to distinguish it from the chaotic dynamics of a quantum system.

As this energy quantization has led to complications for describing chaos in terms of wavefunction dynamics, the study has since shifted towards the interaction between classical and quantum systems in order to induce chaotic behaviour of the correlation. More specifically, for a classical system that demonstrates chaotic behaviour, the correspondence between this and the quantum system will still remain and affect the quantum dynamics [30, 33], primarily contained within the associated waves and energies [34]. With this,

one could then consider semiquantum systems where both classical and quantum degrees of freedom exist and can interact [35, 36]. One such case that has recently found success is the helium atom in determining its higher energy states. The helium atom can be semiclassically expressed as two independent electrons in orbit within the potential of the nucleus, with additional corrections resulting from the electron-electron interactions affecting the Rydberg series of eigenenergies, discussed in Chapter 42 of [16]. These effectively cause a separation between the higher-order energy levels, with this divergence behaving chaotically. Many other systems of this category are often described in terms of oscillators, where a quantum oscillator and classical oscillator are coupled together in such a way that they are able to interact with one another [36, 37]. With this in mind, the simplest quantum-classical interacting system that is often considered takes the Hamiltonian form [36, 37]

$$H = \frac{1}{2}\left[\frac{P_x^2}{m_q} + \frac{p_y^2}{m_c} + m_q\omega^2 X^2\right] \tag{3.4}$$

where P_x and X are quantum operators, y is the classical position, and p_y is the associated classical momentum. This form results from the interaction between a classical oscillator of mass m_c with a quantum oscillator of mass m_q, where the interaction term is held within the frequency [36, 37]

$$\omega^2 = \omega_q^2 + e^2 y^2 \ , \tag{3.5}$$

where e is a parameter to quantify the strength of the system coupling.

While the classical behaviour remains in the form of a stable oscillator, chaotic trends may arise due to interactions with the quantum oscillator. Such an effect can be seen for example in the occupation number of the system, which for this specific case as a fermionic system is restricted to be ≤ 1 [36, 38]. By increasing the resolution to observe narrow bands of momentum, the average occupation number can fluctuate in such a way that it depends heavily on the initial conditions of the system [36]. Additionally, by altering the

system in such a way that the classical limit displays chaos, transitioning the region towards a purely quantum system will restrict the usual description of behaviour to display stable trends [37]. This investigation of semiquantum chaos has also been expanded to double well [35] and triple well potential systems [39] where in each case, the description of chaos remains focused on the correlation between the classical and quantum degrees of freedom.

3.2 Operator Growth and Krylov Complexity

As the interactions between quantum and classical systems have been observed to affect the coupled behaviour, the question still remains as whether chaos can possess its own description in a purely quantum system. In order to describe dynamics in terms of purely quantum aspects of a system, a popular candidate lies in descriptions in terms of the quantum operators and their time-evolution. This operator evolution can then be treated in a similar manner to classical trajectories, with a similar description in terms of a quantum Lyapunov exponent. To understand this further, there must first be a specific description of what is exactly being measured in this quantum Lyapunov exponent in terms of operator growth.

A common choice for measurement of this operator growth is described in terms of the out-of-time-order correlator (OTOC) [40–43]. In order to define this, it is important to note that this description relies on the use of the Heisenberg picture so that the operator contains time-evolution rather than the Schrodinger picture that attributes the time-evolution to the state. In this picture, the time-dependent operator is expressed as [6, 9, 12, 40]

$$O(t) = e^{iHt} O e^{-iHt} \ . \tag{3.6}$$

Considering then two generic time-dependent operators $W(t)$ and $V(t)$, the behaviour of

their commutation relation leads to the definition of the OTOC with [40, 41]

$$C(t) = -\langle [W(t), V(0)]^2 \rangle \tag{3.7}$$

by taking the average of the commutator squared. For a more physical interpretation, one may choose the two operators as X and P_x so that the OTOC becomes

$$C(t) = -\langle [X(t), P_x(0)]^2 \rangle \ . \tag{3.8}$$

In order to understand the behaviour of the OTOC, consider the relation between the commutator and Poisson brackets with $[X, P_x] = i\hbar\{x, p\}$. For a semiclassical limit that exhibits chaos as $e^{\lambda t}$, the OTOC will then grow as $C(t) \propto e^{2\lambda t}$ where the quantum Lyapunov exponent can then be read from λ [41, 42]. From this, the motivation for the OTOC to become a description of quantum chaos has become quite popular as it quantifies chaos in terms of a quantum Lyapunov exponent, analogous to the classical Lyapunov exponent. While not maintaining the definition of chaos in terms of trajectories, it remains a similar understanding with a purely quantum-mechanical description in terms of operators.

The quantum Lyapunov exponents can also be computed via 'scrambling', where an observer is not able to distinguish between a perturbed and unperturbed state when given access to less than half of the system's degrees of freedom [44]. While these systems may not necessarily lose the information of their initial states, an observer with limited information may not be able to form appropriate distinctions. The time required for this limit to be reached is then referred to as the scrambling time t_* [44–46], where the quantum Lyapunov exponents are related to the scrambling time as [44, 46]

$$\lambda = 1/t_* \ . \tag{3.9}$$

Furthermore, for a quantum, bosonic, many-body thermal system of temperature T, this can be bounded as [46, 47]

$$\lambda \leq 2\pi T \ . \tag{3.10}$$

With this relation between quantum Lyapunov exponents and temperature, the OTOC has found considerable application in holography [44, 48–50] along with black hole thermodynamics [51, 52] in order to determine a more clear understanding of the role of chaos in other quantum systems.

While this investigation of the OTOC has found significant success and is continuing to improve, it has not solved every problem with quantum chaos as there remains some discrepancy when translating to classically chaotic systems. In fact for certain cases, the OTOC will not demonstrate positive exponential growth for a classically chaotic system [41, 53]. Inversely, it has also been shown to demonstrate exponential growth when the classical system shows no chaotic behaviour [54–56]. This has since led to an alternate description of operator growth referred to as Krylov complexity to measure the complexity of an operator's evolution [53, 57–59]. In order to understand this new definition, one must first introduce a new operator $\mathcal{L}$, referred to as the Liouvillian superoperator, that acts on other quantum operators. For some operator O, $\mathcal{L}$ then acts on it as [53, 58–60]

$$\mathcal{L}O = [H, O] \ , \tag{3.11}$$

where H is the Hamiltonian. With this operation, the time-dependence of an operator can then be expressed as [53, 59, 60]

$$O(t) = \sum_{n=0}^{\infty} \frac{(it)^n}{n!} \mathcal{L}^n O \tag{3.12}$$

where n is the number of operations of the Liouvillian. This operator expansion appears

similar to a Schrödinger-like equation, where the operator $O(t)$ plays the role of a wavefunction with state vectors expressed in terms of Liouvillian operations $|\tilde{O}_n\rangle = \mathcal{L}^n O$ [58, 60]. The Krylov basis can then be formed through the orthonormalization of these state vectors, using the Lanczos algorithm for the basis [53,57–61]. With these Krylov basis vectors $|O_n\rangle$ as the orthonormal versions of $|\tilde{O}_n\rangle$, the state can be expressed as

$$|O(t)\rangle = e^{i\mathcal{L}t}|O_0\rangle = \sum_n i^n \phi_n(t)|O_n\rangle \ , \tag{3.13}$$

where $\phi_n(t)$ are the amplitudes of the wavefunctions within the Krylov basis [57,58,60,61]. With the normalization condition $\sum_n |\phi_n(t)|^2 = 1$, the Krylov complexity for an operator can be expressed as

$$K(t) = \sum_n n|\phi_n(t)|^2 \ , \tag{3.14}$$

and as n refers to the number of operations of $\mathcal{L}$, this Krylov complexity can approximately measure the number of nested commutators $[H,\cdot]$ in the operator $O(t)$ [53]. Due to the time-dependence within this complexity function, chaotic behaviour can be described similarly in terms of a quantum Lyapunov exponent $K(t) \propto e^{\lambda t}$ [53], now describing the exponential growth in complexity of an operator resulting from n operations of the Liouvillian.

As for the OTOC measurement of quantum chaos, Krylov complexity has also been considered in the context of field theory and holography [62–65]. This approach has produced significant success in studying chaos as the Krylov complexity has grown in agreement with assumptions for certain chaotic systems previously studied [62]. A weakness still remains however, despite its apparent success in that it takes a new definition of chaos in quantum mechanics than for classical mechanics. It continues to describe chaos in terms of quantum operators rather than analogous trajectories, and while it agrees with the expected behaviour of operator complexity, it remains a separate understanding of that for classical chaos. When considering this separation between classical and quantum chaos, perhaps it

is nothing more than a misinterpretation of the quantum phenomena rather than a physical effect. In that case, embracing an alternate interpretation of quantum mechanics may yield a new description of quantum chaos to closer resemble the classical description.

Chapter 4

Bohmian Mechanics

As quantum measurements are commonly described in terms of wavefunction collapse and probability [6, 12], a common criticism arises in that there seems to be no precise description of the intermediate physical behaviour of a quantum system [66]. The focus lies instead on the expectation values, and their corresponding probabilities, resulting from the measurement process rather than the description of the underlying quantum behaviour that gives rise to the measurement itself. This lack of description of the fundamental quantum behaviour becomes so extreme that the expectation value of a measurement cannot even be understood as the value before the measurement even occurred [66, 67] but takes meaning solely after the measurement has been performed, essentially creating the question of whether its existence is dependent on this observation itself. As this underlying behaviour cannot (yet) be scientifically observed, this allows for various interpretation of the occurring phenomena, so long as their predictions do not contradict measurements and observations.

With this motivation for a description of quantum phenomena, David Bohm developed an alternative interpretation for quantum theory [66, 68], often referred to as 'Bohmian Mechanics', by considering a wavefunction $\psi = \mathcal{R}e^{i\mathcal{S}/\hbar}$ where $\mathcal{R} = \mathcal{R}(\vec{r},t)$ and $\mathcal{S} = \mathcal{S}(\vec{r},t)$ are real functions. As derived from the Schrödiner equation (see Appendix A), this quantum system would then be under the influence of some classical background potential and an additional 'quantum potential'

$$V_Q = \frac{-\hbar^2}{2m}\frac{\nabla^2\mathcal{R}}{\mathcal{R}}\,, \tag{4.1}$$

and with the velocity field $\vec{v} = \vec{\nabla}\mathcal{S}/m$, the 'quantum equation of motion' arises in the form

of Newton's second law

$$m\frac{d\vec{v}}{dt} = -\vec{\nabla}(V + V_Q) \tag{4.2}$$

resulting directly from the 'quantum Hamilton-Jacobi equation'

$$0 = \frac{\partial \mathcal{S}}{\partial t} + \frac{(\vec{\nabla}\mathcal{S})^2}{2m} + V + V_Q \, . \tag{4.3}$$

With this quantum equation of motion describing the behaviour of a quantum system, it then follows that this behaviour would have a similar description to a classical system as the equations of motion are of an extremely similar form. As a classical system is described in terms of trajectories resulting from the classical equation of motion, it follows that this quantum equation of motion would then describe behaviour in terms of trajectories, with the standard classical trajectories resulting from the classical background potential now augmented by 'Bohmian trajectories' resulting similarly from the quantum potential [66, 69, 70]. These Bohmian trajectories will generally serve as $O(\hbar^2)$ corrections to the classical trajectories due to the $\hbar^2$ dependence contained within the definition of the quantum potential. As the velocity field $\vec{v} = \vec{\nabla}\mathcal{S}/m$ is clearly dependent on the phase $\mathcal{S}$, and $\mathcal{S}$ is present in the quantum Hamilton-Jacobi equation from Eq. (4.3), then the phase $\mathcal{S}$ has also been referred to as the 'generator of trajectories' as in [70] and Chapter 14 of [12].

Based on the expression of the quantum equation of motion and the description of quantum behaviour in terms of Bohmian trajectories, this formalism provides one of the clearest representations for the classical limit of quantum mechanics. In this limit where the effects of the quantum potential reduce to the point that they become negligible, that is $V_Q \to 0$ [12, 71, 72], the classical equations of motion return and are represented in the form of Newton's second law, as well as the classical Hamilton-Jacobi equation [12, 66, 71–74]. With the quantum potential effectively vanishing in this limit then the Bohmian trajectories resulting from this potential will vanish as well, removing any quantum behaviour from the

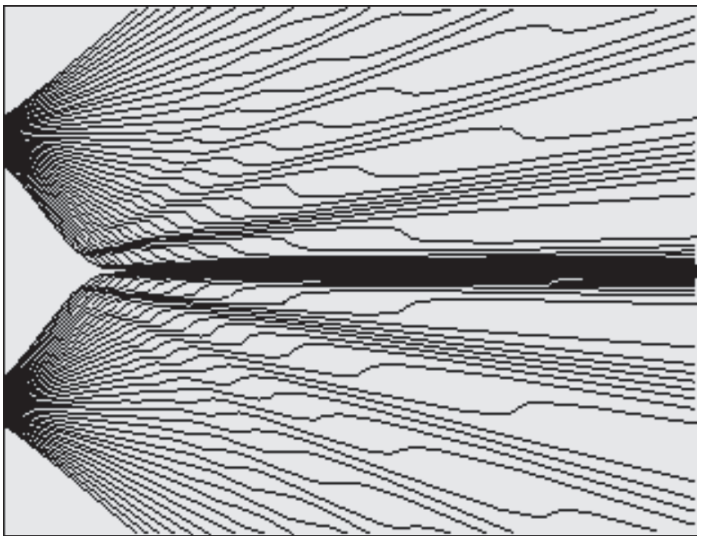

Figure 4.1: The Bohmian trajectories of particles through a double slit apparatus. Reprinted from [3].

observable phenomena and resulting in classically observable behaviour of the system. In the standard quantum limit however, these Bohmian trajectories can be considered as the source of quantum behaviour. In fact, these Bohmian trajectories are capable of describing the results of one of the best known experiments, namely Young's Double Slit experiment [75]. The interference pattern associated with particles passing through an apparatus with two slits takes the form expected when passing waves through the same apparatus, resulting in one of the first experimental proofs of the wave-particle duality associated with quantum theory. By considering the quantum potential and resulting Bohmian trajectories, this interference pattern can be recreated in terms of the trajectories of particles through these slits in response to the quantum potential, rather than the wave-like behaviour of a quantum system [10, 73] as presented in Fig. (4.1). While this is a relatively simple example of quantum behaviour, it clearly demonstrates the capability of the quantum potential in explaining behaviour that had little to no well-expressed description previously.

With this description of quantum behaviour in terms of trajectories in the Bohmian

picture, one could question the role of Heisenberg's uncertainty principle [11]

$$\Delta X \Delta P_x \geq \frac{\hbar}{2} \tag{4.4}$$

as these trajectories may appear as a well-defined position and momentum for any point along the trajectory. This can result in two conclusions for these contradicting descriptions: either the uncertainty principle is not a physical restriction and results from an incomplete theory of quantum mechanics, or these Bohmian trajectories are not continuously observable without influencing the system. In order for these Bohmian trajectories to describe the observable phenomena resulting from quantum theory as it relates to measurable uncertainty, it then leads to the restriction that these Bohmian trajectories must not be observable [68, 76]. Otherwise the uncertainty principle would be violated, despite evidence to the contrary [77]. Therfore, the descriptions in terms of 'trajectories' may be slightly misleading as these are not mapping out the precise path that the particle is travelling over, but are simply the integral curves of the quantum-corrected Newton's law in Eq. (4.2).

One could also make the argument that the uncertainty principle will be originally, and possibly unintentionally, encoded within the Bohmian picture of quantum mechanics based on its original derivation through the Schrödinger equation, and therefore the Bohmian trajectories cannot violate the uncertainty principle. In the standard coordinate representation of quantum mechanics, the momentum operator takes the form $P_x = -i\hbar\frac{\partial}{\partial x}$ and results in the standard commutator relation $[X, P_x] = i\hbar$ [6, 9, 12]. This commutator relation can then directly result in the Heisenberg uncertainty principle as expressed in Eq. (4.4). As this momentum operator is found directly in the Schrödinger equation as expressed in Eq. (3.2), then the uncertainty principle must already be a consideration as it is implied within the momentum operator P_x. Since the Bohmian interpretation is based off of the quantum potential as derived by the Schrödinger equation which automatically implies the Heisenberg uncertainty principle, the Bohmian interpretation cannot violate an implication of its

original derivation. Therefore, the description of quantum behaviour in terms of Bohmian trajectories must not violate this uncertainty, so these Bohmian trajectories must not be continuously observable as a result. In fact, the uncertainty arises in this interpretation as a more practical result from the interaction between the apparatus and the system. In the process of successive measurements on the system, the apparatus itself may introduce additional disturbances that alter the state of the system, resulting in the inability to exactly anticipate or manipulate both the precise position and momentum of the particle simultaneously. This then leads to the position and momentum of the particle to be effectively hidden from the observer during the measurement process, leading to their descriptions as 'hidden variables' [66, 68].

While these properties of the quantum potential are significant in providing a conclusive description of quantum behaviour as it has been observed, one of its strongest advantages arise in its classical limit when describing motion [12, 73]. As briefly mentioned previously (and in Appendix A), the quantum equations of motion approach the classical equations of motion in the limit of $V_Q \to 0$, where in the classical limit, this quantum potential will effectively vanish and be removed from the quantum equations of motion. The resulting quantum Hamilton-Jacobi equation and quantum equation of motion will only change in that the quantum potential will be removed, and therefore will simply result in the classical Hamilton-Jacobi equation and Newton's second law respectively. Additionally, the Bohmian trajectories would no longer result from the quantum form of Newton's second law, with only the standard classical trajectories remaining. With these effects, the interpretation of quantum mechanics in terms of Bohm's quantum potential produces a clearer description of the classical limit resulting in the standard observations of classical mechanics with any quantum variations reducing in magnitude and effectively vanishing from observation.

Chapter 5

A New Description of Quantum Chaos

Since the Bohmian formulation of quantum mechanics predicts the presence of Bohmian trajectories as $O(\hbar^2)$ corrections to the standard classical trajectories, and chaos in classical mechanics is studied in terms of trajectories, it follows that these Bohmian trajectories would provide a clear motivation for studying chaos in the realm of quantum mechanics. Additionally, as the classical limit of quantum mechanics is perhaps expressed most clearly in the Bohmian picture, the behaviour of these Bohmian trajectories may provide further insight into chaotic behaviour of the corresponding classical trajectories in the limit when quantum mechanical effects can be ignored.

This idea can be realized as a direct result of the quantum equation of motion as expressed in Eq. (4.2), where the 'total' potential V_{tot} seen by a quantum particle is the sum of the background classical potential (V) and a wavefunction-dependent quantum potential (V_Q). There is no way for the particle to distinguish between the two potentials, or tell which fraction of the total potential is classical and which is quantum. It follows therefore that one of the above potentials, or the entirety, can be fully substituted by the other without the particle having any indication. This provides a unique advantage that every classical potential that gives rise to chaos can now be entirely replaced by a quantum potential, created by a suitable wavefunction, as long as this quantum potential takes an identical form to the previous classical potential so that the resulting equations of motion are identical. Therefore it follows that the quantum particle will behave equally chaotically, but now as a result of a purely quantum effect as opposed to a classical one. It is this behaviour that will be examined further in the two examples to follow. Additionally, as it is purely the amplitude

of the wavefunction which determines the required quantum potential, it may appear that there is a considerable degree of freedom in choosing its phase. However, note that since the velocity field $\vec{v} = \vec{\nabla}\mathcal{S}/m$ is clearly dependent on the phase $\mathcal{S}$ as present in the quantum Hamilton-Jacobi equation Eq. (4.3), it is in turn determined by the effective equation of motion from Eq. (4.2) and will therefore hold the description of the Bohmian trajectories.

5.1 The Parametric Oscillator

To test if such a wavefunction can exist in principle in order to create a quantum potential as described above, consider one of the simplest cases of classical chaos, namely the parametric oscillator in one dimension as discussed in Section 2.2.

Following the above motivation for replacing any classical potential by an equivalent quantum potential, consider a 'free' particle such that $V = 0$, but now subjected to a quantum potential of the same form, namely

$$V_Q = \frac{1}{2}k\left[1 + h\cos(\gamma t)\right]x^2 \,. \tag{5.1}$$

Recall that it is the slowly varying time-dependent frequency as expressed in Eq. (2.5) (whose variation itself is determined by the quantity γ) which gives rise to the phenomenon of chaos in this system. Furthermore, from the definition of the quantum potential as presented in Eq. (4.1), this time-dependence can effectively be treated as a constant in the context of the quantum potential as it involves only partial derivatives with respect to space. As a result, the amplitude of the wavefunction $\mathcal{R}$ responsible for the quantum potential must satisfy the partial differential equation

$$\frac{\partial^2}{\partial x^2}\mathcal{R} + bx^2\mathcal{R} = 0 \tag{5.2}$$

where $b = \frac{mk}{\hbar^2}[1 + h\cos(\gamma t)]$, obtained simply by re-arranging Eq. (4.1) with V_Q given by Eq. (5.1).

To solve this for $\mathcal{R}$, consider a power series solution for a differentiable equation of the form

$$\mathcal{R} = \sum_{n=0}^{\infty} a_n x^{n+s} \, . \tag{5.3}$$

Following the procedure from Appendix B, the final solution for the wavefunction amplitude can be displayed most clearly as a linear sum of series $\mathcal{R} = \mathcal{R}_1 + \mathcal{R}_2$, where $\mathcal{R}_1$ and $\mathcal{R}_2$ are even and odd series respectively[3], with

$$\mathcal{R}_1 = \sum_{n=0}^{\infty} (-1)^n b^n c_n x^{4n} \qquad \mathcal{R}_2 = \sum_{n=0}^{\infty} (-1)^n b^n d_n x^{4n+1} \, , \tag{5.4}$$

$$c_n = \frac{c_{n-1}}{4n(4n-1)} \qquad d_n = \frac{d_{n-1}}{4n(4n+1)} \, . \tag{5.5}$$

As each successive coefficient c_n and d_n result directly from recurrence relations as expressed in Eq. (5.5), the wavefunction amplitudes $\mathcal{R}_1$ and $\mathcal{R}_2$ will become dependent on c_0 and d_0 respectively. Additionally, any relevant initial conditions of the system can be encoded into these coefficients along with the required coefficients resulting from the linear combination of $\mathcal{R}_1 + \mathcal{R}_2$. However, as these conditions are not essential to describe the general behaviour of the wavefunction amplitude and will only effect the magnitude of the amplitude, they can be left as arbitrary here.

Next, one must check that the solution is finite at every point in space. This can be done by checking the convergence of the series using the ratio test [78]. The radius of

[3] At the conclusion of this exercise, it was realized that this could be written in terms of hypergeometric functions. In principle, this analysis could then be done in terms of these hypergeometric functions, which as it would likely not yield any new results, is left as a future exercise.

convergence for the series solutions $\mathcal{R}_1$ and $\mathcal{R}_2$ can be expressed respectively as

$$|x^4| < \lim_{n\to\infty} \left| \frac{4n(4n-1)}{b} \right| \tag{5.6}$$

and

$$|x^4| < \lim_{n\to\infty} \left| \frac{4n(4n+1)}{b} \right| . \tag{5.7}$$

As both these limits reduce to $|x| < \infty$, the radius of convergence for both series is infinite and therefore the wavefunction amplitude will converge to a finite value over the entire space. This result can be checked with an additional convergence test, namely the Cauchy root test [78], where the radius of convergence for $\mathcal{R}_1$ and $\mathcal{R}_2$ are represented respectively as

$$|x^4| < \lim_{n\to\infty} \left| \frac{1}{b\sqrt[n]{c_n}} \right| \tag{5.8}$$

and

$$|x^4| < \lim_{n\to\infty} \left| \frac{1}{b\sqrt[n]{d_n x}} \right| . \tag{5.9}$$

Using the definitions of c_n and d_n from Eq. (5.5), these limits too reduce to $|x| < \infty$, and therefore the wavefunction amplitude will again converge over the entire region of x in $(-\infty, \infty)$. With two separate convergence tests producing the same region of convergence $|x| < \infty$, one can be more confident that the wavefunction exists and will converge to a finite value for any value of x.

With these tests completed, the general requirements must then be satisfied in that the wavefunction amplitude $\mathcal{R}$ and its derivative $\partial\mathcal{R}/\partial x$ be continuous. As the wavefunction amplitude is expressed as a power series from Eq. (5.4), its derivative will then take the form of a power series with slightly modified coefficients and powers of x with

$$\frac{\partial \mathcal{R}}{\partial x} = \sum_{n=1}^{\infty} (-1)^n b^n \left[4nc_n x^{4n-1} + (4n+1) d_n x^{4n} \right] . \tag{5.10}$$

This derivative clearly exists as a real function, as well as being continuous as it remains as a polynomial of order $n \to \infty$ with no clear discontinuity for any value of x in $(-\infty, \infty)$. With these two conditions, the wavefunction amplitude remains a valid and potentially physical solution.

Finally, in order for this wavefunction amplitude to have any physical significance, it must be normalizable so that probability is conserved. Assuming that the original wavefunction amplitude solution $\mathcal{R}$ is not yet normalized, consider the normalized amplitude

$$\tilde{\mathcal{R}} = \frac{\mathcal{R}}{\sqrt{N}} \tag{5.11}$$

that conserves the probability of the system. This then depends on the normalization coefficient N, defined as

$$N = \int_{-L}^{L} \mathcal{R}^2 dx \tag{5.12}$$

which depends on the region of normalization for x in $(-L, L)$. As this normalization coefficient N is calculated using the square of a series, this can become extremely difficult to express explicitly, but it becomes much simpler when the series in Eq. (5.12) is expanded to a finite number of terms and studied numerically. Using a simple *Mathematica* code, N can be written as another power series where the coefficients again depend on a recurrence relation with decreasing magnitude as $n \to \infty$, where each term is a multiple of either c_0^2 or d_0^2. For simplicity, these coefficients can be expressed as $f(n)c_0^2$ or $g(n)d_0^2$ where the functions $f(n)$ and $g(n)$ represent the decreasing nature of the coefficients, and are directly related to the definitions of c_n and d_n respectively from Eq. (5.5). With these functions, the normalization coefficient can then be computed and expressed in a general form as

$$N = \sum_{n=0}^{\infty} (-1)^n b^n \left\{ f(n) c_0^2 L^{4n+1} + g(n) d_0^2 L^{4n+3} \right\} . \tag{5.13}$$

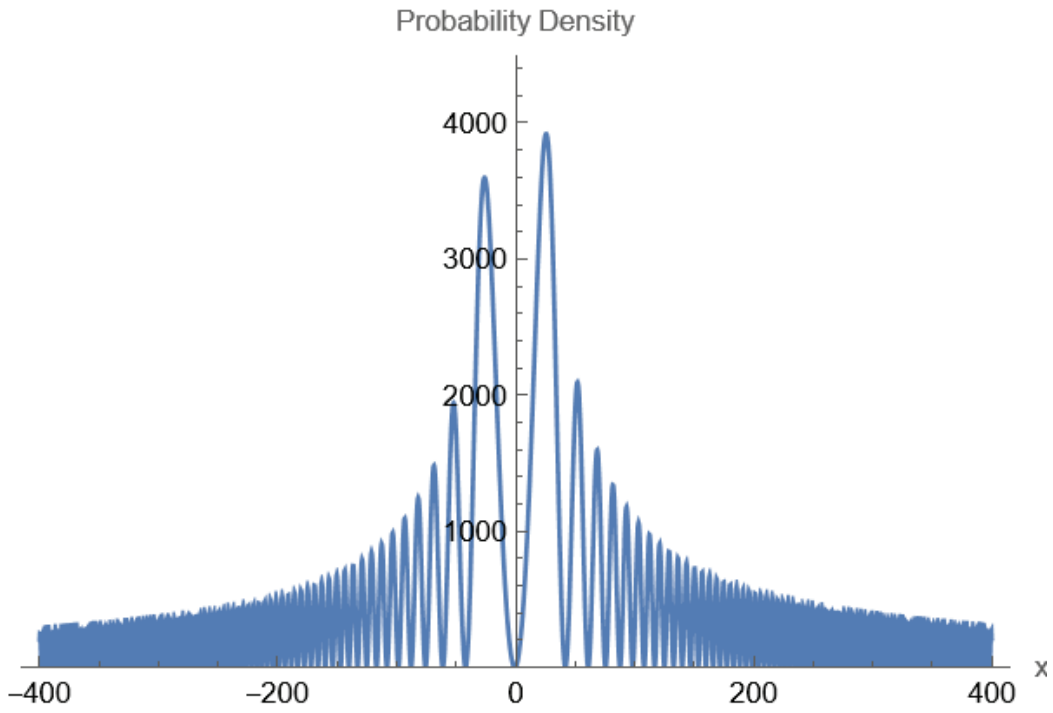

Figure 5.1: The probability distribution $|\mathcal{R}|^2$ of the wavefunction required to produce a quantum potential to mimic the parametric oscillator.

As this normalization coefficient is some finite value for any finite L, then the wavefunction amplitude is normalizable. Due to the power series form for the normalization coefficient, it is not clear as to how the wavefunction amplitude will behave under the limit $L \to \infty$ in relation to the coefficient functions $f(n)$ and $g(n)$, as these may approach the limit of $1/\infty$ faster than $L \to \infty$ and will therefore dominate the behaviour of the system. Due to the complexity in computing and expressing these functions explicitly, consider instead the numerical solutions to represent the system within some region of finite L. By choosing arbitrary values of $c_0 = 2$ and $d_0 = 3$ as they will only affect the magnitude of the amplitude rather than its behaviour, taking the series expansion to $n = 600$ terms, and $b = 10^{-5}$ to decrease the width of each peak in order to view the general trend of the function within an observable region of x, the probability distribution $|\mathcal{R}|^2$ can be plotted using *Mathematica* to observe its behaviour as the range increases. As displayed in Fig. (5.1), the probability distribution shows a general decrease in magnitude as the range increases, leading to the conclusion that the coefficient functions $f(n)$ and $g(n)$ will decrease faster than the depen-

dence on x with an assumption that this will continue as $x \to \infty$. As this is quite complicated to show analytically, and numerical solutions are limited to finite values of x, this trend may not continue with complete certainty and the wavefunction amplitude will be restricted to box-normalization rather than normalization over the entire region of x in $(-\infty, \infty)$.

With the effort spent on normalizing the wavefunction, a concern can arise as to how this may impact the quantum potential, as there was no consideration of normalization previously. Based on the definition of the quantum potential as expressed in Eq. (4.1), the second-order partial derivative of $\mathcal{R}$ will not change the form of the normalization coefficient, and it will then cancel as a result of the amplitude-dependent fraction. In other words, the quantum potential is independent of the overall normalization of any wavefunction! This will hold true for the even, odd or a representative combination of those wavefunctions

$$\tilde{\mathcal{R}} = \begin{cases} \frac{1}{\sqrt{N_1}} \mathcal{R}_1 \\ \frac{1}{\sqrt{N_2}} \mathcal{R}_2 \\ \frac{1}{\sqrt{N_{12}}} (\mathcal{R}_1 + \mathcal{R}_2) \end{cases} \tag{5.14}$$

where N_1, N_2, and N_{12} are the normalization coefficients for the wavefunction amplitudes $\mathcal{R}_1$, $\mathcal{R}_2$, and $\mathcal{R}_1 + \mathcal{R}_2$ respectively.

With this valid wavefunction, which can in principle be generated in a suitable laboratory environment, consider next the behaviour of a particle described by a wavefunction with this particular amplitude in Eq. (5.14), or more specifically, in the absence of any classical background potential where the resulting quantum potential is of the form of the parametric oscillator. The resulting Bohmian trajectories from this potential will behave exactly as the classical trajectories resulting from the parametric oscillator since this quantum potential takes the exact form of the classical parametric oscillator potential. As this system has been extensively studied and observed as chaotic in classical mechanics, as discussed in

Section 2.2, the Bohmian trajectories must follow this same chaotic behaviour as their classical counterparts. Since this chaotic behaviour is a result of the strength of the perturbation from the simple harmonic oscillator as determined by the parameter h, and contained within the coefficient b in the solution for the wavefunction amplitude in Eq. (5.4), it follows that any chaotic behaviour demonstrated by these Bohmian trajectories will be a direct result of the wavefunction. Since this wavefunction provides the only influence on these Bohmian trajectories, this chaotic behaviour must be a purely quantum effect! It can be argued that this is an alternate and convenient way of looking at quantum chaos, especially for certain systems, and may complement the existing formulations of quantum chaos.

5.2 The Hénon-Heiles Hamiltonian

As a suitable wavefunction was found as a physically valid solution when working in one dimension, the next concern arises as to whether this procedure can be replicated with increasing degrees of freedom. With this in mind, consider next a similar two-dimensional system that has been observed as being chaotic in classical mechanics, namely, the Hénon-Heilies Hamiltonian as discussed in Section 2.3. As was the case for the parametric oscillator discussed previously, consider a quantum potential to replace the classical Hénon-Heiles potential as represented and discussed in Eq. (2.8), such that

$$V_Q = \frac{1}{2}k(x^2+y^2) + h\left(x^2y - \frac{1}{3}y^3\right) \ . \tag{5.15}$$

This quantum potential is clearly more complicated than the parametric oscillator as its definition from Eq. (4.1) will result in a two-dimensional partial differential equation, which then results in significantly more complicated solution methods. With this motivation, consider the slightly rearranged form of the differential equation in Eq. (5.15) with

$$-\frac{\hbar^2}{2m}\nabla^2\mathcal{R} + F(x,y)\mathcal{R} = 0 \ , \tag{5.16}$$

where $F(x,y) = -V_Q$ in order to recognize equations of a similar form that have more well-known methods for solutions. As expected, this does appear similar to a well-known partial differential equation, namely the Schrödinger equation. By considering the Schrödinger equation in the presence of a classical background potential

$$-\frac{\hbar^2}{2m}\nabla^2\psi + V(x,y)\psi = -i\hbar\frac{\partial}{\partial t}\psi \tag{5.17}$$

but with $\frac{\partial}{\partial t}\psi = 0$, then Eq. (5.16) would be expected to have solutions of a similar form and procedure, though slightly modified. Due to the complexity of the function $F(x,y) = -V_Q$, as well as the inherent difficulty when considering a two-dimensional partial differential equation, numerical analysis is often the primary focus for methods of solution.

To complete this numerical analysis, consider the Lanczos algorithm [79] as implemented by [80] to solve for the ground state wavefunction solutions to the Schrödinger equation for various background potentials. These (continuous) wavefunctions are solved using a discrete numerical approximation such that evolution can be considered as steps of $\psi(x\pm 1, y\pm 1)$, and by applying closed boundary conditions such that the wavefunction only exists within the confines of the potential. In the case that the wavefunction returns a finite value over the entire domain, these boundary conditions will automatically result in a box-normalized wavefunction since the computation cannot consider the entire region of x, y in $(-\infty, \infty)$. By modifying the original code [80], solutions for the wavefunction amplitude in Eq. (5.16) can be found for the chosen quantum potential to observe if the resulting probability distributions both exist and are normalizable. The first case of consideration takes $h = 0$ so that the quantum potential takes the form of a simple harmonic oscillator. The resulting wavefunction amplitude would then be expected to take the form of a Gaussian peak centered at $x, y = 0$ as discussed in Chapter 5 of [6]. As shown in Fig. (5.2), both the quantum potential and probability distribution behave as expected, where the probability distribution clearly exists and is normalizable. As expected, it also shows a stable solution.

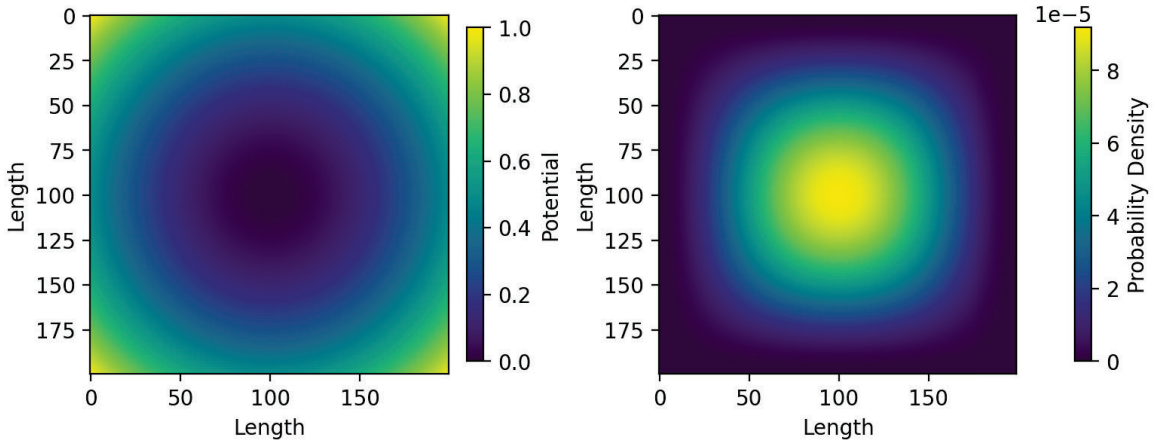

Figure 5.2: The quantum potential to mimic the Hénon-Heiles potential and resulting wavefunction probability distribution, with $k = 1$, $h = 0$, and $m, \hbar = 1$.

By increasing the magnitude of h to mimic the classically chaotic system, one can observe the effect it has on the graph, in terms of the resultant wavefunction and the related quantum potential. In other words, one sees that such a wavefunction and potential indeed exist.

With this goal in mind, consider the next case where $k = h = 1$ so that there is no immediately clear term that dominates the behaviour of the system. As shown in Fig. (5.3), the potential has been modified such that the single well has been perturbed to a more triangular-like well. Despite this change, the overall behaviour would still remain stable as expected from Fig. (2.4). The probability distribution however does not appear to be modified, or more likely, modified so slightly that the changes are not distinguishable. From this form, the probability density again clearly exists and is normalizable. The resulting Bohmian trajectories would then exhibit stable behaviour as they would take the form of the classical trajectories of a simple harmonic oscillator, with slight perturbations.

Next we consider the other extreme situation, namely when the cubic perturbation term dominates, and the behaviour of the system differs greatly from the harmonic oscillator.

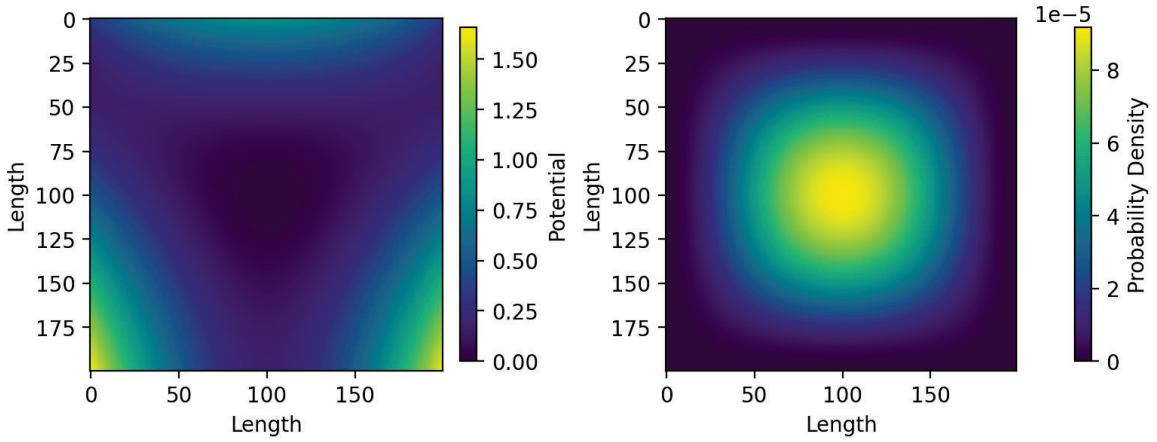

Figure 5.3: The quantum potential to mimic the Hénon-Heiles potential and resulting wavefunction probability distribution, with $k = 1$, $h = 1$, and $m, \hbar = 1$.

With parameters $k = 1$ and $h = 50$, the quantum potential shown in Fig. (5.4) can be seen to mimic the Hénon-Heiles potential as represented originally in Fig. (2.3) as there is no longer a clearly defined potential well. The probability distribution created by the wavefunction amplitude also differs from the previous cases as the once centralized peak has been modified to an approximately triangular shape. Despite the change in shape, it remains box-normalizable for a finite region of space so the wavefunction amplitude remains possible as a physical solution. Additionally, the Bohmian trajectories that result from this quantum potential will clearly behave in a similar manner to the classical trajectories from the original Hénon-Heiles potential as discussed in Section 2.3. As before, just as the classical trajectories exhibit chaotic behaviour, these Bohmian trajectories must also exhibit this same chaotic behaviour as dictated by the quantum equation of motion in Eq. (4.2).

As the wavefunction amplitude has been shown to result in probability distributions that exist and are normalizable over some finite region of space, then it can in principle be generated in a suitable laboratory. As this wavefunction amplitude was specifically chosen to produce a quantum potential to mimic the Hénon-Heiles potential which has been observed

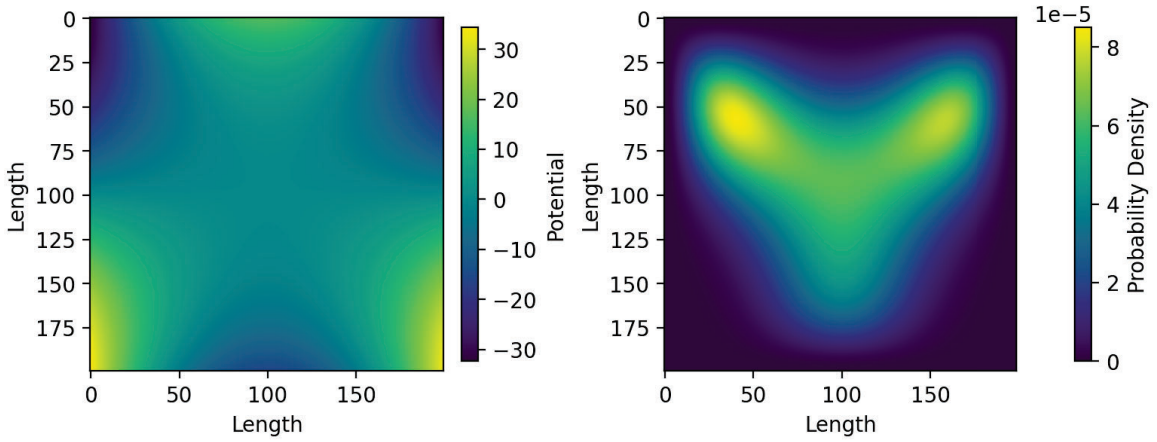

Figure 5.4: The quantum potential to mimic the Hénon-Heiles potential and resulting wavefunction probability distribution, with $k = 1$, $h = 50$, and $m, \hbar = 1$.

to produce classical trajectories that exhibit chaotic behaviour, the Bohmian trajectories resulting from this potential must behave similarly and will therefore behave chaotically. Additionally, as this potential takes the form of a perturbed two-dimensional harmonic oscillator with the strength of the perturbation determined by the parameter h, and h as found in the quantum potential would have to arise within the wavefunction amplitude, then the chaotic behaviour of these Bohmian trajectories would result directly from the quantum wavefunction, and therefore can be considered as a form of quantum chaos.

Having studied in detail two systems in which chaos is described in terms of the behaviour of Bohmian trajectories, one may argue that this is a start of an alternate and simple approach to studying quantum chaos. For any quantum potential, whether chosen to produce chaotic trajectories or not, the required wavefunction may be solved in order to describe the system quantum mechanically. The stipulation remains that the wavefunction amplitude must be solvable as a real function as well as being (box-)normalizable, and as this has not been proven to be the case for a quantum potential of any imaginable form, this claim cannot be made with absolute certainty. Regardless, the initial success of this method

calls for further consideration of this new description of chaos in terms of the Bohmian trajectories as influenced by the wavefunction.

5.3 Comparison of Quantum Chaos Descriptions

With this new understanding of quantum chaos in terms of Bohmian trajectories and the quantum potential, there is a clear discussion as to whether this may provide a more beneficial description. The answer to this may not be a completely clear choice or unanimously agreed upon, but the potential benefits of this new description should call for some level of consideration.

The first, and most clear, distinction between this new description and the common descriptions is the understanding of chaos in terms of trajectories. A description of quantum chaos in terms of Bohmian trajectories as determined by Eq. (4.2) draws a clear correspondence to classical chaos in terms of classical trajectories. Additionally, the description of Bohmian trajectories as $O(\hbar^2)$ corrections to the classical trajectories gives a clear result of classical chaos as a limit of quantum chaos as $\hbar \to 0$. This then provides support for the standard interpretation of Bohr's correspondence principle, which has been questioned by some as a result of the common descriptions of quantum chaos [13]. The previous understandings of quantum chaos as described in terms of energy levels and operator growth lacked a clear description of the classical limit of these behaviours despite studying the behaviour relating to classically chaotic systems. However, this new description holds the standard interpretation of classical behaviour as a limit of quantum behaviour as well as providing a new way to interpret quantum chaotic dynamics.

This does however provide a new limit of understanding as it requires one to adopt Bohmian Mechanics as an alternate formulation of quantum mechanics rather than the standard Copenhagen interpretation that is considered and taught most commonly. Rather

than describing the measurement process in terms of operations causing the collapse of the wavefunction, the observations in Bohmian Mechanics arise as a measurement at some point along the Bohmian trajectory as determined by the quantum potential. This does not invalidate any previously observed quantum phenomena, but rather explains it in an alternate way, likely causing a certain level of skepticism as it goes against the standard interpretations. However, as the Bohmian interpretation produces the same observable results as for the Copenhagen interpretation, this should not become a major criticism for the results as discussed in the previous chapter.

Instead, more significant subjects for debate lie in the interpretation of the previous results as 'quantum chaos'. As in the common descriptions of quantum chaos, the primary descriptions focus on the time-evolution of quantum operators as counterparts to classical trajectories. In this new description however, the understanding of quantum chaos takes a similar description to classical chaos as they both work in terms of trajectory divergence, but using Bohmian and classical trajectories respectively. The potential for disagreement lies in the interpretation and physical representation, or lack thereof, of these Bohmian trajectories since they have been shown to describe quantum phenomena but are not physically observable. While this may immediately sound like a substantial obstacle, it could be argued that this is no more alarming than the representation in terms of operators for the common descriptions of quantum chaos. The final state(s) of a quantum system can be observable, despite the effects resulting from trajectories or operators, with the intermediate behaviour lacking a concrete description as the measurements themselves will alter the system. By considering the behaviour of the operators, or more specifically the time-evolution as described in the Heisenberg picture, the effects of the operators on the wavefunction can again only be described in terms of final and initial states. This can still be a sufficient description of chaos as it focuses on the divergence between final and initial states, essentially being blind to the intermediate behaviour, but this again provides no clear advantage over

this new description in terms of Bohmian trajectories. The final effects produce the only observable behaviour in both cases, with the intermediate interpretation being the only differing property. Essentially, the final conclusions from a quantum system are independent of the picture making this a perfectly valid choice for description!

On the other hand, this new description may hold an advantage based on its 'universality' in describing chaotic systems. By allowing the quantum potential to hold the relevant descriptions of behaviour in a quantum system, then perhaps the only restriction that can be placed is whether the determining wavefunction is a valid wavefunction. The quantum potential could take the effective form of any classically chaotic potential, and the Bohmian trajectories would behave exactly the same as that in the classical system. This could then allow for any number of quantum chaotic systems as long as they mimic the classical counterparts, and the chaotic behaviour will already be well understood in the quantum system as it would mimic the classical system. This may not be as simple in practice however, as it may prove difficult to observe physical quantum systems with a wavefunction of the exact form as required for the specific quantum potential.

Chapter 6
Conclusion

In order to describe the universe from its smallest to largest length scales, one could justifiably expect a general description of phenomena to exist that covers every applicable scale. Therefore, such a description would be expected to describe both classical and quantum behaviour within their respective length scales. This would also imply potential for a smooth transition between the classical and quantum behaviour at intermediate length scales.

Examples of classically chaotic behaviour were shown in Chapter 2 as they describe the behaviour of classical trajectories, where trajectories were generally considered as chaotic if they displayed extreme sensitivity to the initial conditions of the system. These sensitivities can be represented both quantitatively and qualitatively in Section 2.1 through the use of Lyapunov exponents and Poincaré plots respectively.

When comparing this description of chaos to quantum mechanics however, there emerges a disagreement as quantum mechanics, as it is commonly interpreted, leaves no room for trajectories. In Section 3.2, quantum chaos was described in its common methods using the OTOC and Krylov complexity. These methods however rely on a description in terms of quantum operators rather than trajectories, so there appears to be some level of disagreement towards a universal description of chaos at every length scale. As this appears to violate Bohr's correspondence principle, one could justifiably call for a reinterpretation of either quantum chaos or the correspondence principle. Choosing the former, and considering the interpretation of quantum mechanics in terms of the quantum potential and resulting

Bohmian trajectories as explained in Chapter 4, one could describe quantum chaos in terms of Bohmian trajectories to create a closer correspondence to classical chaos.

In this work (Chapter 5), this alternate interpretation of quantum mechanics was implemented by choosing specific quantum potentials to mimic the classically chaotic potentials as discussed in Sections 2.2 and 2.3. With these potentials, and the definitions of the quantum potential in Eq. (4.1), the corresponding wavefunction amplitudes were solved in both cases to be real and (box-)normalizable. This then implies that these wavefunctions may be generated in a suitable laboratory or even exist naturally. Additionally, as these wavefunctions would produce a quantum potential of the exact form of a classically chaotic potential, the Bohmian trajectories would behave chaotically in the exact manner as the analogous classical trajectories. Therefore, as this chaotic behaviour of the Bohmian trajectories is a direct result of the wavefunction amplitude, this would be a purely quantum form of chaos.

Due to the formulation of Bohmian Mechanics in that it provides a description of classical behaviour as a limit of quantum mechanics, this new interpretation may also provide additional insight for its classical limit. Consider a system that contains classical trajectories, with additional Bohmian trajectories presenting as $O(\hbar^2)$ perturbations. If one was able to tune the system, with sufficient accuracy, then perhaps the transition could be observed as the classical trajectories begin to feel the effect of these quantum perturbations. This could shed new light on the classical or quantum dominance at intermediate length scales, as well as providing an understanding of the validity of taking $\hbar \to 0$ as the classical limit or if there is additional dependence on other factors. One can also maintain the description of Bohr's correspondence principle in such a limit in order to approach a single understanding of mechanics, both classical and quantum, within the same theory.

This is however a new approach to quantum chaos, so there is still a fair amount of work to do for a complete picture of this interpretation. The first task would be to address the phase of the wavefunction. While it is only the amplitude that effects the form of the quantum potential, it is the phase that contains to relevant description of the Bohmian trajectories as observed in the quantum Hamilton-Jacobi equation in Eq. (4.3). For the two previously considered systems, each phase should be found to ensure that it accurately describes the system as well presenting as a real function, as required in the formulation of Bohmian Mechanics (see Chapter 4 and Appendix A). With this, the wavefunction of each system can be explained in its entirety to ensure that all requirements are met. Additionally, this approach should be taken to a variety of classically chaotic potentials to ensure that this interpretation of quantum chaos holds for a variety of systems and that these were not fortunate but outlying cases. With a more expansive collection of wavefunctions for quantum chaotic systems, it may also be possible to identify key features of both the amplitude and phase that may hint at chaotic behaviour resulting from the wavefunction and avoiding a more thorough analysis of the system.

6.1 Final Remarks

As two specific quantum potentials were shown to result from physically valid wavefunctions, and the resulting Bohmian trajectories would behave chaotically as for the corresponding classical system, then this behaviour should be classified as quantum chaos. By comparing this description to the common descriptions of quantum chaos, this approach can be very practical as it clearly resembles the description of classical chaos. Additionally, given the form of these Bohmian trajectories as perturbations to the classical trajectories, this may become a useful tool in understanding the classical limit of quantum mechanics and the transition between classical and quantum behaviour.

Bibliography

[1] V.L. Berdichevsky and M.v. Alberti. Statistical Mechanics of Hénon-Heiles oscillators. *Physical Review A*, 44:858–865, 1991.

[2] M. Hénon and C. Heiles. The Applicability of the Third Integral of Motion: Some Numerical Experiments. *The Astronomical Journal*, 69(1):73–79, 1964.

[3] Wikimedia Commons. Surreal electron trajectories in two-slit experiment according to Bohmian mechanics, 2005. https://commons.wikimedia.org/wiki/File:Surreal.gif.

[4] I. Newton. *Philosophiæ Naturalis Principia Mathematica*. 1687.

[5] M. Planck. *Verhandlungen der Deutschen Physikalischen Gesellschaft*, volume 2. 1900.

[6] R. Shankar. *Principles of Quantum Mechanics*. Springer, 2nd edition, 1994.

[7] C.-D. Yang and S.-Y. Han. Trajectory Interpretation of Correspondence Principle: Solution of Noda Issue. *Foundations of Physics*, 50:960–976, 2020.

[8] S. Fortin and O. Lombardi. The Correspondence Principle and the Understanding of Decoherence. *Foundations of Physics*, 49:1372–1393, 2019.

[9] N. Zettili. *Quantum Mechanics: Concepts and Applications*. Wiley, 2nd edition, 2009.

[10] P.R. Holland. *The Quantum Theory of Motion*. Cambridge University Press, 1993.

[11] W. Heisenberg. Ueber den anschaulichen Inhalt der quantentheoretischen Kinematik and Mechanik. *Zeitschrift für Physik*, 43(3-4):172–198, 1927.

[12] L.E. Ballentine. *Quantum Mechanics: A Modern Development*. McGraw-Hill, 2nd edition, 2014.

[13] R.W. Batterman. Chaos, quantization, and the correspondence principle. *Synthese*, 89(2):189–227, 1991.

[14] S.T. Thornton and J.B. Marion. *Classical Dynamics of Particles and Systems*. Brooks/Cole, 5th edition, 2004.

[15] H. Goldstein, C.P. Poole, and J.L. Safko. *Classical Mechanics*. McGraw-Hill, 3rd edition, 2002.

[16] P. Cvitanović, R. Artuso, R. Mainieri, G. Tanner, and G. Vattay. *Chaos: Classical and Quantum*. ChaosBook.org, 17th edition, 2023.

[17] K.T. Alligood, T.D. Sauer, and J.A. Yorke. *Chaos: An Introduction to Dynamical Systems*. Springer, 1st edition, 1996.

[18] P.B. Persson and C.D. Wagner. General principles of chaotic dynamics. *Cardiovascular Research*, 31(3):332–341, 03 1996.

[19] K.-E. Thylwe and H.J. Korsch. Harmonic oscillator subject to parametric pulses: an amplitude (Milne) oscillator approach. *Journal of Physics A: Mathematical and General*, 34(16):3497, 2001.

[20] F. Verhulst. *Encyclopedia of Complexity and Systems Science*. 2009. https://api.semanticscholar.org/CorpusID:18845183.

[21] B. Ftorek, P. Orsanský, and H. Samajová. Parametric oscillations of the mechanical systems. *MATEC Web of Conferences*, 157:08002, 2018.

[22] R. Kawai, K. Lindenberg, and C. Van den Broeck. Parametrically modulated oscillator dimer: an analytic solution. *Physics A: Statistical Mechanics and its Applications*, 312:0119–140, 2002.

[23] L. D. Landau and E. M. Lifshitz. *Mechanics: Volume 1 (Course of Theoretical Physics)*. Butterworth-Heinemann, 3rd edition, 1976.

[24] C. Klausmeier. Lyapunov Exponent [Online Discussion Post]. *Mathematica Stack Exchange*, Aug 2022. https://mathematica. stackexchange.com/questions/17593/lyapunov-exponent/179470#179470.

[25] E. Bolcal, C. Karakus, and Y. Polatoglu. Analyzing the Chaotic Behaviour of the Harmonic Function of Henon-Heiles Potential. *Springer Chaos and Complex Systems*, pages 459–468, Jan 2013.

[26] E.E. Zotos. An overview of the escape dynamics in the Hénon–Heiles Hamiltonian system. *Meccanica*, 52(11), 2017.

[27] S. Alhowaity, E.I. Abouelmagd, Z. Diab, and J.L.G. Guirao. Calculating periodic orbits of the Hénon-Heiles system. *Frontiers in Astronomy and Space Sciences*, 9, 2023.

[28] E. Chan-López'. Evaluating the Poincaré section for Hénon-Heiles potential through Hénon Method [Online Discussion Post]. *Mathematica Stack Exchange*, Jun 2023. https://mathematica.stackexchange.com/questions/204648/evaluating-the-poincaré-section-for-hénon-heiles-potential-through-hénon-method.

[29] R.V. Jensen. Quantum Chaos. *Nature*, 355:311–318, 1992.

[30] G. Casati. Quantum Chaos. *Chaos: An Interdisciplinary Journal of Nonlinear Science*, 6(3):391–398, 1996.

[31] D. Lassoued and M. Fečkan. Boundedness and almost periodicity of solutions of linear differential systems. *Mathematica Slovaca*, 72(5):1203–1214, 2022.

[32] M.V. Berry, I.C. Percival, and N.O. Weiss. The Bakerian Lecture, 1987. Quantum chaology. *Proceedings of the Royal Society of London. A. Mathematical and Physical Sciences*, 413(1844):183–198, 1987.

[33] A.D. Stone. Einstein's Unknown Insight and the Problem of Quantizing Chaos. *Physics Today*, 58(8):37–43, 08 2005.

[34] M.A. Porter. An Introduction to Quantum Chaos. *arXiv: Chaotic Dynamics*, 2001.

[35] T.C. Blum and H.-T. Elze. Semiquantum chaos in the double well. *Physical Review E*, 53:3123–3133, Apr 1996.

[36] F. Cooper, J.F. Dawson, D. Meredith, and H. Shepard. Semiquantum chaos. *Physical Review Letters*, 72:1337–1340, Feb 1994.

[37] A.M. Kowalski, M.T. Martin, J. J Nuñez, A. Plastino, and A.N. Proto. Semiquantum chaos and the uncertainty principle. *Physica A: Statistical Mechanics and its Applications*, 276(1):95–108, 2000.

[38] K. Stowe. *An Introduction to Thermodynamics and Statistical Mechanics*. Cambridge University Press, 2nd edition, 2007.

[39] T.O. Lekeufack, S.B. Yamgoue, and T.C. Kofane. Signature of chaos in the semi quantum behavior of a classically regular triple well heterostructure. *Natural Science*, 02(03):145–154, 2010.

[40] I. García-Mata, R.A. Jalabert, and D.A. Wisniacki. Out-of-time-order correlators and quantum chaos. *Scholarpedia*, 18:55237, 2023.

[41] K. Hashimoto, K. Murata, and Y. Ryosuke. Out-of-time-order correlators in quantum mechanics. *Journal of High Energy Physics*, 2017(138), 2017.

[42] D.A. Trunin. Refined quantum Lyapunov exponents from replica out-of-time-order correlators. *Physical Review D*, 108:105023, 2023.

[43] T. Zhou and B. Swingle. Operator growth from global out-of-time-order correlators. *Nature Communications*, 14:3411, 2023.

[44] H.R. Hampapura, A. Rolph, and B. Stoica. Scrambling in two-dimensional conformal field theories with light and smeared operators. *Physical Review D*, 99:106010, May 2019.

[45] S. Khetrapal. Chaos and operator growth in 2d CFT. *Journal of High Energy Physics*, 2023(176), 2023.

[46] S. Das, B. Ezhuthachan, A. Kundu, S. Porey, B. Roy, and K. Sengupta. Out-of-Time-Order correlators in driven conformal field theories. *Journal of High Energy Physics*, 2022(221), 2022.

[47] J. Maldacena, S.H. Shenker, and D. Stanford. A bound on chaos. *Journal of High Energy Physics*, 2016(106), 2016.

[48] S. Giombi, S. Komatsu, and B. Offertaler. Chaos and the reparametrization mode on the AdS_2 string. *Journal of High Energy Physics*, 2023(23), 2023.

[49] N. Bao and N. Cheng. Eigenstate thermalization hypothesis and approximate quantum error correction. *Journal of High Energy Physics*, 2019(152), 2019.

[50] A. Bagchi, S. Chakrabortty, D. Grumiller, B. Radhakrishnan, M. Riegler, and A. Sinha. Non-Lorentzian chaos and cosmological holography. *Physical Review D*, 104:L101901, Nov 2021.

[51] B. Craps, S. Khetrapal, and C. Rabideau. Chaos in CFT dual to rotating BTZ. *Journal of High Energy Physics*, 2021(105), 2021.

[52] J. de Boer, E. Llabrés, J.F. Pedraza, and D. Vegh. Chaotic Strings in AdS/CFT. *Physical Review Letters*, 120:201604, May 2018.

[53] K. Hashimoto, K. Murata, and R. Watanabe. Krylov complexity and chaos in quantum mechanics. *Journal of High Energy Physics*, 11(40), 2023.

[54] T. Xu, T. Scaffidi, and X. Cao. Does Scrambling Equal Chaos? *Physical Review Letters*, 124:140602, Apr 2020.

[55] K. Hashimoto, K.-B. Huh, K.-Y. Kim, and R. Watanabe. Exponential growth of out-of-time-order correlator without chaos: inverted harmonic oscillator. *Journal of High Energy Physics*, 2020(68), 2020.

[56] A. Bhattacharyya, W. Chemissany, S. Shajidul Haque, J. Murugan, and B. Yan. The multi-faceted inverted harmonic oscillator: Chaos and complexity. *SciPost Phys. Core*, 4:002, 2021.

[57] D.E. Parker, X. Cao, A. Avdoshkin, T. Scaffidi, and E. Altman. A Universal Operator Growth Hypothesis. *Physical Review X*, 9:041017, Oct 2019.

[58] C. Liu, H. Tang, and H. Zhai. Krylov complexity in open quantum systems. *Physical Review Research*, 5:033085, Aug 2023.

[59] M. Alishahiha and S. Banerjee. A universal approach to Krylov state and operator complexities. *SciPost Physics*, 15:080, 2023.

[60] K. Adhikari, S. Choudhury, and A. Roy. Krylov Complexity in Quantum Field Theory. *Nuclear Physics B*, 993:116263, 2023.

[61] E. Rabinovici, A. Sánchez-Garrido, R. Shir, and J. Sonner. Krylov complexity from integrability to chaos. *Journal of High Energy Physics*, 2022(151), 2022.

[62] A. Dymarsky and M. Smolkin. Krylov complexity in conformal field theory. *Physical Review D*, 104:L081702, Oct 2021.

[63] A. Kundu, V. Malvimat, and R. Sinha. State dependence of Krylov complexity in 2d CFTs. *Journal of High Energy Physics*, 2023(11), 2023.

[64] E. Rabinovici, A. Sánchez-Garrido, R. Shir, and J. Sonner. A bulk manifestation of Krylov complexity. *Journal of High Energy Physics*, 2023(213), 2023.

[65] P. Caputa and S. Datta. Operator growth in 2d CFT. *Journal of High Energy Physics*, 2021(188), 2021.

[66] D. Bohm. A Suggested Interpretation of the Quantum Theory in Terms of "Hidden" Variables. I. *Phys. Rev.*, 85:166–179, Jan 1952.

[67] A. Einstein. Quantum Mechanics and Reality. *Dialectica*, 2(3-4):320–324, 1948.

[68] D. Bohm. A Suggested Interpretation of the Quantum Theory in Terms of "Hidden" Variables. II. *Phys. Rev.*, 85:180–193, Jan 1952.

[69] S. Das and S. Sourav. On the quantum origin of potentials. *The European Physical Journal Plus*, 137, Dec 2021.

[70] S. Das. Quantum Raychaudhuri equation. *Phys. Rev. D*, 89:084068, Apr 2014.

[71] A.O. Bolivar. The bohm quantum potential and the classical limit of quantum mechanics. *Canadian Journal of Physics*, 81(7):971–976, 2003.

[72] G.E. Bowman. On the Classical Limit in Bohm's Theory. *Foundations of Physics*, 35(4):605–625, 2005.

[73] C. Philippidis, C. Dewdney, and B.J. Hiley. Quantum interference and the quantum potential. *Il Nuovo Cimento B*, 52:15–28, 07 1979.

[74] U. Klein. What is the limit $\hbar \to 0$ of quantum theory? *American Journal of Physics*, 80(11):1009–1016, 2012.

[75] T. Young. The Bakerian Lecture. Experiments and calculations relative to physical optics. *Philosophical Transactions*, 94:1–16, 1804.

[76] S. Aristarhov. Heisenberg's Uncertainty Principle and Particle Trajectories. *Foundations of Physics*, 53, 2023.

[77] W. Ma, Z. Ma, H. Wang, Z. Chen, Y. Liu, F. Kong, Z. Li, X. Peng, M. Shi, F. Shi, S. Fei, and J. Du. Experimental Test of Heisenberg's Measurement Uncertainty Relation Based on Statistical Distances. *Physical Review Letters*, 116(16), 2016.

[78] D. Zwillinger. *CRC Standard Mathematical Tables and Formulae*. CRC Press LLC, 2003.

[79] C. Lanczos. An Iteration Method for the Solution of the Eigenvalue Problem of Linear Differential and Integral Operators. *Journal of Research of the National Bureau of Standards*, 45(4), 1950.

[80] W. Longtin and K. Surrao. Solving the Schrödinger equation computationally using the Lanczos algorithm. *Journal of Emerging Investigators*, 6, 2023.

[81] K. F. Riley, M. P. Hobson, and S. J. Bence. *Mathematical Methods for Physics and Engineering: A Comprehensive Guide*. Cambridge University Press, 3rd edition, 2006.

Appendix A

Bohmian Mechanics as Derived from the Schrödinger Equation

Following the procedure as used in David Bohm's original formulation [66, 68], consider a complex wavefunction in polar form $\psi = \mathcal{R}e^{i\mathcal{S}/\hbar}$ where $\mathcal{R} = \mathcal{R}(\vec{r},t)$ and $\mathcal{S} = \mathcal{S}(\vec{r},t)$ are restricted to real functions. Substituting this wavefunction into the Schrödinger equation, maintaining generality in a $(n+1)$-dimensional spacetime, the equation becomes simply

$$\frac{-\hbar^2}{2m}\nabla^2\left(\mathcal{R}e^{i\mathcal{S}/\hbar}\right) + V\left(\mathcal{R}e^{i\mathcal{S}/\hbar}\right) = i\hbar\frac{\partial}{\partial t}\left(\mathcal{R}e^{i\mathcal{S}/\hbar}\right) . \tag{A.1}$$

Due to the wavefunction being a complex function, it follows that the Schrödinger equation will result in two relations, one for the real parts and another for the imaginary parts. To see these relations more clearly, consider the expanded form for each term within Eq. (A.1). The first term can be expanded as a result of the Laplacian operator as

$$\frac{-\hbar^2}{2m}\nabla^2\left(\mathcal{R}e^{i\mathcal{S}/\hbar}\right) = \left[\frac{-\hbar^2}{2m}\nabla^2\mathcal{R} - \frac{i\hbar}{m}(\vec{\nabla}\mathcal{R})\cdot(\vec{\nabla}\mathcal{S}) - \frac{i\hbar}{2m}\mathcal{R}\nabla^2\mathcal{S} + \frac{1}{2m}\mathcal{R}(\vec{\nabla}\mathcal{S})^2\right]e^{i\mathcal{S}/\hbar} , \tag{A.2}$$

the second term will remain unchanged as the potential V will not affect the wavefunction, and the third term can be expanded as

$$i\hbar\frac{\partial}{\partial t}\left(\mathcal{R}e^{i\mathcal{S}/\hbar}\right) = \left[i\hbar\frac{\partial\mathcal{R}}{\partial t} - \mathcal{R}\frac{\partial\mathcal{S}}{\partial t}\right]e^{i\mathcal{S}/\hbar} . \tag{A.3}$$

By substituting these expanded terms back into Eq. (A.1), and cancelling out the exponential function from every term, the Schrödinger equation will take the form

$$\frac{-\hbar^2}{2m}\nabla^2\mathcal{R} - \frac{i\hbar}{m}(\vec{\nabla}\mathcal{R})\cdot(\vec{\nabla}\mathcal{S}) - \frac{i\hbar}{2m}\mathcal{R}\nabla^2\mathcal{S} + \frac{1}{2m}\mathcal{R}(\vec{\nabla}\mathcal{S})^2 + V\mathcal{R} = i\hbar\frac{\partial\mathcal{R}}{\partial t} - \mathcal{R}\frac{\partial\mathcal{S}}{\partial t}\,. \quad \text{(A.4)}$$

As expected, this can clearly be represented in terms of the real and imaginary parts, with

$$\frac{-\hbar^2}{2m}\left[\nabla^2\mathcal{R} - \frac{\mathcal{R}}{\hbar^2}(\vec{\nabla}\mathcal{S})^2\right] + V\mathcal{R} = -\mathcal{R}\frac{\partial\mathcal{S}}{\partial t} \quad \text{(A.5)}$$

and

$$\frac{1}{2m}\left[\mathcal{R}\nabla^2\mathcal{S} + 2(\vec{\nabla}\mathcal{R})\cdot(\vec{\nabla}\mathcal{S})\right] = -\frac{\partial\mathcal{R}}{\partial t} \quad \text{(A.6)}$$

respectively.

In order to understand the full description of this system as a result of the Schrödinger equation, each resulting relation should be investigated further to understand their implications. Beginning with the relation between the real parts, Eq. (A.5) can be simply rearranged to take the form

$$0 = \frac{\partial\mathcal{S}}{\partial t} + \frac{(\vec{\nabla}\mathcal{S})^2}{2m} + V - \frac{\hbar^2}{2m}\frac{\nabla^2\mathcal{R}}{\mathcal{R}}\,. \quad \text{(A.7)}$$

As this takes the form of the Hamilton-Jacobi equation [15] in the limit of $\hbar \to 0$, then this can essentially be understand as a 'quantum Hamilton-Jacobi equation' [12] for $\hbar \neq 0$. With the form of the Hamilton-Jacobi equation, each particle can be observed to be under the influence of both the classical potential V and this additional potential, referred to as the 'quantum potential' [66]

$$V_Q \equiv \frac{-\hbar^2}{2m}\frac{\nabla^2\mathcal{R}}{\mathcal{R}}\,. \quad \text{(A.8)}$$

To understand the behaviour of a particle under these potentials V and V_Q, consider the

gradient of Eq. (A.7) with a velocity field $\vec{v} = (\vec{\nabla}\mathcal{S})/m$, resulting in

$$\begin{aligned} 0 &= \frac{\partial}{\partial t}(\vec{\nabla}\mathcal{S}) + \frac{1}{m}(\nabla^2\mathcal{S})(\vec{\nabla}\mathcal{S}) + \vec{\nabla}(V + V_Q) \\ &= m\left[\frac{\partial \vec{v}}{\partial t} + (\vec{v}\cdot\vec{\nabla})\vec{v}\right] + \vec{\nabla}(V + V_Q) \\ &= m\frac{d\vec{v}}{dt} + \vec{\nabla}(V + V_Q) \\ \Rightarrow\ m\frac{d\vec{v}}{dt} &= -\vec{\nabla}(V + V_Q) \end{aligned} \tag{A.9}$$

which is clearly Newton's second law of motion, with the classical potential term augmented by the addition of the quantum potential V_Q.

As the real parts of the Schrödinger equation contain the description of the motion and behaviour of the quantum system, it follows that the imaginary parts must also contain some relevant description for some properties of the quantum system. To investigate this further, Eq. (A.6) can be rewritten by introducing an additional factor of $\mathcal{R}$ and combining terms for

$$0 = \vec{\nabla}\cdot\left(\frac{\mathcal{R}^2\vec{\nabla}\mathcal{S}}{m}\right) + \frac{\partial}{\partial t}(\mathcal{R}^2)\ . \tag{A.10}$$

From the definition of the probability density $\rho = |\psi|^2 = \mathcal{R}^2$ and the probability flux [12] $\vec{J} = \frac{\mathcal{R}^2\vec{\nabla}\mathcal{S}}{m}$, then this can be simply written as

$$0 = \vec{\nabla}\cdot\vec{J} + \frac{\partial \rho}{\partial t}\ , \tag{A.11}$$

which is nothing more than the conservation of probability.

Appendix B

Series Solutions for the Wavefunction Amplitude

In order to solve Eq. (5.2) for a general wavefunction amplitude, consider the Frobenius method of series solutions for a differential equation [81]. This assumes a solution of the form

$$\mathcal{R} = \sum_{n=0}^{\infty} a_n x^{n+s} \tag{B.1}$$

with the first and second order derivatives following as

$$\mathcal{R}' = \sum_{n=0}^{\infty} (n+s) a_n x^{n+s-1} \tag{B.2}$$

and

$$\mathcal{R}'' = \sum_{n=0}^{\infty} (n+s)(n+s-1) a_n x^{n+s-2} \ . \tag{B.3}$$

These functions can then be substituted back into the original differential equation (5.2) to return

$$\begin{aligned} 0 &= \sum_{n=0}^{\infty} (n+s)(n+s-1) a_n x^{n+s-2} + b x^2 \sum_{n=0}^{\infty} a_n x^{n+s} \\ &= \sum_{n=0}^{\infty} (n+s)(n+s-1) a_n x^{n+s-2} + b \sum_{n=0}^{\infty} a_n x^{n+s+2} \\ &= \sum_{n=-4}^{\infty} (n+s+4)(n+s+3) a_{n+4} x^{n+s+2} + b \sum_{n=0}^{\infty} a_n x^{n+s+2} \ . \end{aligned} \tag{B.4}$$

To combine these two series into a single series, both summations must cover the same range of n. To that end, the first series can be partially expanded so that the $-4 \leq n \leq -1$

terms appear outside of the series and both can begin at $n = 0$, resulting in

$$\begin{aligned} 0 = {} & s(s-1)a_0x^{s-2} + (s+1)sa_1x^{s-1} + (s+2)(s+1)a_2x^s + (s+3)(s+2)a_3x^{s+1} \\ & + \sum_{n=0}^{\infty} [(n+s+4)(n+s+3)a_{n+4} + ba_n]x^{n+s+2} \ . \end{aligned} \tag{B.5}$$

The indicial equation can now be recovered by setting the coefficients of each term to 0, with the first term resulting in

$$0 = s(s-1)a_0 \ . \tag{B.6}$$

Two roots can be easily found from this as $s_1 = 0$ and $s_2 = 1$. As these roots differ by an integer, with the integer difference holding for every other term in the series, choosing either root solution will yield the same expansion. Choosing the $s = 0$ root, the series expansion can be simplified to

$$0 = 2a_2 + 6a_3x + \sum_{n=2}^{\infty} [(n+2)(n+1)a_{n+2} + ba_{n-2}]x^n \ . \tag{B.7}$$

With this final form for the series expansion, the behaviour of the coefficients can now be analyzed in more detail to understand the final form for the solution $\mathcal{R}$. The coefficients of x^0 and x^1 can be read directly from Eq. (B.7) $a_2 = a_3 = 0$. For additional powers of x^n for $n \geq 2$, Eq. (B.7) results in a recurrence relation as

$$a_{n+4} = \frac{-ba_n}{(n+4)(n+3)} \tag{B.8}$$

following from a slight modification to investigate the terms as $n \geq 0$ rather than its original expression in relation to $n \geq 2$. By solving this for several terms of increasing n, this recurrence relation will produce two separate series with the terms of even n all depending on a_0, and the terms of odd n depending on a_1. Combining both series into a single expression

for $\mathcal{R}$ produces

$$\begin{aligned}\mathcal{R} &= a_0 + a_1 x - \frac{b}{12} a_0 x^4 - \frac{b}{20} a_1 x^5 + \frac{b^2}{56(12)} a_0 x^8 + \frac{b^2}{72(20)} a_1 x^9 - \ldots \\ &= a_0 \left[1 - \frac{b}{12} a_0 x^4 + \frac{b^2}{56(12)} a_0 x^8 - \ldots \right] + a_1 \left[x - \frac{b}{20} a_1 x^5 + \frac{b^2}{72(20)} a_1 x^9 - \ldots \right] \\ &= \sum_{n=0}^{\infty} (-1)^n b^n \left(c_n x^{4n} + d_n x^{4n+1} \right)\end{aligned} \tag{B.9}$$

with

$$c_n = \frac{c_{n-1}}{4n(4n-1)} \tag{B.10}$$

and

$$d_n = \frac{d_{n-1}}{4n(4n+1)} \, , \tag{B.11}$$

where c_0 and d_0 are determined from the boundary conditions of the system.